Elucidation of physiological factors regulating height growth of conifer trees

Azuma, Wakana

(Degree)
博士（農学）

(Date of Degree)
2016-03-25

(Date of Publication)
2017-03-01

(Resource Type)
doctoral thesis

(Report Number)
甲第6658号

(URL)
https://hdl.handle.net/20.500.14094/D1006658

Doctoral Dissertation

博士論文

Elucidation of physiological factors regulating height growth of conifer trees

針葉樹の樹高成長を規定する生理学的要因の解明

Wakana Azuma

東　若菜

January 2016
Graduate School of Agricultural Science, Kobe University
平成 28 年 1 月
神戸大学大学院農学研究科農学研究科

Table of contents

Chapter 1

General introduction

1.1 Background

1.1.1 Ecological and practical significance of tree height

Tree height is an important variable for ecology and forestry. For example, as stand biomass increases in direct proportion to height (Tsutsumi 1989), maximum tree height defines productivity of forest ecosystems. Site index, which represents potential forest stand productivity, is evaluated by the height of upper canopy trees at 40-years stand age (Iwatsubo 1996). Site index is an integrative concept expressing the general production capacity of a forest stand, it is the outcome of various environmental and physiological factors and the result of stand growth, and it is not a predictive index. If the physiological mechanisms regulating maximum tree height are revealed, we may be able to predict potential stand productivity from the measurement of environment conditions, such as soil condition and climatic condition. Besides, stand productivity, CO_2 fixation by forests is considered an important carbon sink for preventing global warming. As the amount of CO_2 fixation by a tree is defined by how tall the tree grows, revealing the physiological mechanisms regulating maximum tree height is important for accurate predictions of the amount of CO_2 fixation by forest ecosystems.

Recently in Japan, long-rotation forestry is applied increasingly in stand management. However, long-term predictions of primary production is still lacking, particularly of stands older than the conventional harvesting age. In terms of conservation ecology, old-growth trees is valuable for both cultural and biological conservation. However, concerning old-growth trees, physiological growth mechanisms and biomass accumulation is still not well understood.

In general, forests comprising various tree species have high leaf area index (LAI; total leaf area of whole plant per unit land area) and large stand biomass (Hiura 2001). As light

transmittance from canopy to ground changes with developing crown structure, various tree species with different maximum heights coexist along the gradient of light availability, resulting in light-use complementarity and increasing community-level diversity and productivity (Gravel et al. 2010). Within individual trees, phenotypic plasticity, such as branch spatial arrangement and leaf/shoot morphology changes with vertical gradient of light availability within canopy, which result in increased light-use efficiency and tree-level productivity (Leverenz and Hinckley 1993; Ishii et al. 2013). Therefore, it is important for understanding ecological function of whole forest ecosystem to focus on individual phenotypic plasticity and elucidate a perspective of canopy ecophysiology.

1.1.2 Previous studies of tree height growth in tall trees

"What is the factor determining the limit to tree height?" is an old and considerably debated question. Physiological studies of tree height growth has been conducted on tall conifers in the North American West Coast (e.g., Koch et al. 2004). The hydraulic limitation hypothesis (HLH; Ryan and Yoder 1997) is the first, physiology-based theoretical hypothesis based of height growth in tall tree. With increasing tree height, hydrostatics factors such as elongation of the water-transport pathway and gravitational force constrain vertical water transportation from root to treetop, resulting in decreasing xylem water potential (Zimmermann 1983; Bauerle et al. 1999; Midgley 2003). Thus treetop leaves of tall trees easily experience severe water deficit, which triggers decreasing photosynthesis, called water stress. In HLH, constraints on vertical water transport resulting in increasing water stress with increasing height is considered as the limiting factor that constrains physiological function and height growth of tall trees.

Hydrodynamic factors such as high irradiance and transpiration demands at treetop also contribute to increased water stress (Franks 2006). For example, with increasing height, average treetop sap velocity, transpiration per unit leaf area and stomatal conductance per unit leaf area significantly decrease in *Sequoia sempervirens*, the world's tallest existing tree species (Ambrose et al. 2010).

Regardless of photosynthesis, lack of turgor pressure during morphogenesis due to decreasing leaf water potential at the treetop can directly constrain leaf/shoot elongation in tall *Pseudotsuga menziesii* (Woodruff et al. 2004). Generally, leaf morphology become acclimated to light environment (e.g. Niinemets and Kull 1995), but in *Sequoia sempervirens*, treetop leaves do not change their morphology with increasing light availability while proportional changes are observed in relation to height (Ishii et al. 2008). Beyond individual trees, in an old-growth tropical forest which is 20 m of average height, leaf morphology was mainly determined by height, not light availability (Cavaleri et al. 2010). These studies suggest that leaf morphology is affected by water stress, attributable to increasing height, constraining treetop growth.

Conversely, however, a review of 51 studies indicated that physiological functioning does not always decline at the tops of tall trees (Ryan et al. 2006). For example, hydraulic conductance increases at favorable light environment of treetop (e.g. Sellin and Kupper 2005) and a decreasing leaf area: sapwood area ratio adjusts the balances between water demand and water supply (e.g. Burgess et al. 2006; Ambrose et al. 2009). Other compensating mechanisms to overcome the difficulty of water transport from root to treetop are suggested to exist (Zaehle 2005). It seems that mechanisms exist that maintain hydraulic status of leaves in order to sustain physiological function near the treetop where light availability is the greatest for photosynthesis.

1.1.3 Relationships between hydraulic properties and morpho-anatomical traits

As mentioned above, water is closely related to tree height growth. To reveal the physiological mechanisms that determine tree height growth, we should investigate from various scales and aspects. Because hydraulic properties (e.g., hydraulic conductance, capacitance, leaf area: sapwood area ratio, embolism resistance) link to various morphological and anatomical traits (e.g., sapwood area, conduit length, wall thickness, pit anatomy), which affect hydraulic performance (e.g., the amount of water transported per unit time by the bole under specified conditions) of a plant units (a cell, tissue, organ, or whole plant) (Lachenbruch and McCulloh 2014). In previous studies, it was investigated well that xylem structure of stem and branch contribute to their functions such as hydraulic conductance and embolism resistance because stem and branches are the main pathway of water transportation (e.g. Dunham et al. 2007; McCulloh et al. 2010). While leaf hydraulic conductance substantially constrains whole-plant water transport, little is known of its association with leaf structure and function (Sack et al. 2003). Recently, it was found that the density of leaf veins affects leaf hydraulic conductance (Brodribb et al. 2010) and tracheids peripheral of leaf deform under declining leaf hydraulic conductance (Brodribb and Holbrook 2005). To reveal more associations between hydraulic properties and architectural traits helps understanding of hydraulic performance.

On a different note, “water” as defined in tree physiology is a generic term referring to the cluster of water molecules connected by hydrogen bonding. The number of water molecules constituting a cluster can vary from 2 to 600 (Maréchal 2007). A configuration of water molecules interacts their hydrogen bonding, for example, the configuration of ice is a regular array resulting in a uniform short hydrogen bonding, while that of liquid

water has various lengths of hydrogen bonds. Such physicochemical differences of water molecules are considered to affect physiological functions in living systems (Maréchal 2007), but the details of their interaction are not well understood. Considering physicochemical properties of water in tree physiological study can provide a new perspective to plant hydraulics studies.

1.2 Study overview

Chapter 1: Here, I gave an outline of the significance of tree height in forest ecology and forestry, previous studies of tree height growth, and relationships between hydraulic properties and architectural traits. Most conventional hypotheses of height-growth limitation in tall trees have proposed theoretical concepts, e.g., HLH. However, these hypotheses have not been verified rigorously by actual measurements in tall trees.

Chapter 2: I present direct measurements of leaf water relations, the actual level of water stress in leaves of the world's tallest species, *Sequoia sempervirens*. I also investigated the variation in tissue structure of leaves with height, focusing on the relationship with hydraulic properties.

Chapter 3: In order to expand the results of Chapter 2 on various species, the actual level of water stress is also investigated in *Cryptomeria japonica*, the tallest species in Japan. In addition, a detailed anatomical measurement is conducted for leaf tissue to elucidate the associations between hydraulic properties and architectural traits.

Chapter 4: The mechanism of water retention in leaves is investigated from the physicochemical perspective. Infrared micro-spectroscopy is applied to leaves samples of *Cryptomeria japonica* in order to quantify water which exist at various states of hydrogen bonding and visualizing where water is retained in leaf tissue.

Chapter 5: Finally, I provide the study summary and proposes a new hypothesis about regulation of tree height growth.

Chapter 2

Pushing the limits to tree height: could foliar water storage compensate for hydraulic constraints in *Sequoia sempervirens*?

2.1 Abstract

The constraint on vertical water transport is considered an important factor limiting height growth and maximum attainable height of trees. Here, evidence was found that foliar water storage could partially compensate for this constraint in *Sequoia sempervirens*, the tallest species. The hydraulic and morpho-anatomical characteristics of foliated shoots of tall *S. sempervirens* trees were measured near the wet, northern and dry, southern limits of its geographic distribution in California, USA. The ability to store water (hydraulic capacitance) and saturated water content (leaf succulence) of foliage both increased with height and light availability, maintaining tolerance of leaves to water stress (bulk-leaf water potential at turgor loss) constant relative to height. Transverse-sectional area of water-storing, transfusion tissue in leaves increased with height, while the area of xylem tissue decreased, indicating increasing allocation to water storage and decreasing reliance on water transport from roots. Treetop leaves of *S. sempervirens* absorb moisture via leaf surfaces and have potential to store more than five times the daily transpirational demand. Thus, foliar water storage may be an important adaptation that helps maintain physiological function of treetop leaves and hydraulic status of the crown, allowing this species to partially compensate for hydraulic constraints and sustain turgor for both photosynthesis and height growth.

2.2 Introduction

Sequoia sempervirens is the only tree species with living individuals exceeding 100 m in height. The tallest living individual was remeasured at 115.76 m in 2013 (S.C. Sillett unpublished). The physiological mechanisms underlying its incredible height have recently been documented (Koch et al. 2004; Ishii et al. 2008). Water supply to treetop leaves is a key factor determining maximum attainable tree height in *S. sempervirens* (Ambrose, Sillett and Dawson 2009) and other tall species (Ryan, Phillips and Bond 2006; Meinzer et al. 2010). With increasing height, both the distance from roots to leaves and the hydrostatic gradient caused by gravity impose limits on water transport (Midgley 2003). Thus, treetop leaves operate under some minimum constant water stress, constraining important physiological functions, including cell elongation and photosynthesis, and ultimately limiting height growth (Mencuccini et al. 2005; Ryan, Phillips and Bond 2006). Due to these constraints, the estimated maximum attainable height for *S. sempervirens* under current environmental conditions is at least 122 m (Koch et al. 2004; Koch and Sillett 2009). In addition to a limited water supply, drier air and higher temperatures near the treetop caused by high light intensities increase evaporative demand, exacerbating leaf water stress (Franks 2006). This is an inescapable consequence of height, and tall trees must cope with the dilemma that water stress is never alleviated and greatest where light availability for photosynthesis is highest.

The incredible stature of *S. sempervirens* suggests this species may have physiological adaptations that compensate for increasing water stress with height (West, Brown and Enquist 1999; Du et al. 2008), which may include through leaf surfaces (Burgess and Dawson 2004). The tallest individuals occur in moist temperate forests near the species' northern distribution limit in California, where rainfall is abundant and summer fog

occurs frequently (Dawson 1998). In contrast, tree heights are lower in drier regions near the species' southern distribution limit. Absorption of fog via leaf surfaces reduces water stress of *S. sempervirens* leaves, so that leaf water supply does not depend solely on soil water availability and transport from roots (Simonin, Santiago and Dawson 2009). If the absorbed water can be stored in treetop leaves, it would reduce further the reliance on vertical water transport. Although hydraulic capacitance of woody tissue is considered an important internal source of water in large trees (Phillips et al. 2003; Cermak et al. 2007; Scholz et al. 2011), foliar water storage has received less attention (Sack et al. 2003).

A striking feature of *S. sempervirens* is the great variation in shoot/leaf morphology from top to bottom of the crown, which can span more than 90 m in depth (Koch et al. 2004). Treetop leaves are small, thick and fused to the vertically oriented shoot axis. In contrast, lower-crown leaves are large, flat and segregated from the horizontally oriented shoot axis. Generally, acclimation to the vertical gradient in light availability explains changes in leaf morphology within a tree crown (Valladares and Niinemets 2007; Niinemets 2010). In tall trees, however, morpho-anatomical characteristics of leaves are more strongly determined by hydraulic properties associated with height (Marshall and Monserud 2003; Cavaleri et al. 2010; Oldham et al. 2010). In tall *S. sempervirens*, leaf mass per area (LMA) increases with height, leading to less evaporative surface area per unit leaf mass, whereas LMA is not correlated with light intensity above 70 m (Ishii et al. 2008). Leaves of all gymnosperm species have water-storing, transfusion tissue surrounding vascular bundles (Brodribb and Holbrook 2005; Aloni, Foster and Mattsson 2013). Transfusion tissue, first documented in 1864, is a tracheary element composed of tracheids, parenchyma and albuminous cells (Takeda 1913; Hu and Yao 1981). In *S. sempervirens*, the amount of transfusion tissue increases with increasing height, reflecting

anatomical acclimation to increasing water stress (Oldham et al. 2010).

In this study, the hydraulic and morpho-anatomical characteristics of leaves of tall *S. sempervirens* trees were measured near the wet, northern and dry, southern limits of its distribution in California. The object of this study were to investigate how the capacity and mechanisms for foliar water storage respond to increasing water stress associated with increasing height and atmospheric evaporative demand and to discuss how such adaptations may contribute to maintaining hydraulic status in treetop leaves of the world's tallest species.

2.3 Materials and methods

2.3.1 Study site

The study was conducted at Prairie Creek Redwoods State Park (41.37°N, 124.02°W, 55 m asl) and Landels-Hill Big Creek Reserve (36.05°N 121.57°W, 60 m asl). Long-term (1895–2012) average annual precipitation at Prairie Creek is 1857 mm with 55 mm occurring during summer months (June, July and August), whereas Landels-Hill receives 801 mm with only 5 mm occurring in summer (PRISM Climate Group 2013). Based on records from Arcata Airport (40.98°N, 124.11°W, 64 m asl) and Monterey Peninsula Airport, CA (36.58°N, 121.85°W, 50 m asl) located near the two study sites, long-term (1951–2009) averages of fog frequencies (i.e. number of days when visibility <1 km) are 43.5 and 40.5%, respectively, with fog frequencies being highest during summer months (Johnstone & Dawson 2010).

2.3.2 Foliage sampling and measurement of light environment

Three study trees were selected from among the tallest individuals at each site (Table 2.1). The single-rope climbing technique was used to access their crowns and a tape measure was stretched from treetop to ground level. Small branches (30–50 cm long) were sampled from the outer crown of each tree at 10- to 15-m intervals from just below treetop to the lowest living branch.

Hemispherical photographs were taken directly above each sampling location to quantify the light environment. Sample branches were sealed in black plastic bags, transported to the ground, immediately recut under water and fully rehydrated in the laboratory overnight.

2.3.3 Leaf water relations

The bench-drying approach to the pressure–volume technique (Tyree and Hammel 1972; Schulte and Hinckley 1985) to measure bulk-leaf water potential (Ψ_L) and fresh weight (before and after each water potential reading) repeatedly of three to five small, foliated shoots comprising second- and current-year internodes (repeat pressurization method, Hinckley et al. 1980; Ritchie and Roden 1985; Parker and Colombo 1995). Care was taken to increase and decrease the pressure in the chamber very slowly (<0.01 MPa s^{-1}) so as not to damage the sample shoot. During the pressure–volume measurements, when the shoot was slowly pressurized to force water out of the xylem, cases were observed where excess water (i.e. water stored outside of vascular tissue) entered the xylem and bulk-leaf water potential recovered. This effect was corrected for following methods described in Kubiske and Abrams (1991).

The pressure–volume curve was used to calculate fresh weight at saturation (M_F, g), hydraulic capacitance (C, mol m^{-2} MPa^{-1}), osmotic potential at turgor loss (Ψ_{tlp}, MPa) and relative water content at turgor loss (RWC_{tlp}) at the bulk-shoot level (Cheung, Tyree and Dainty 1975; Richter 1978; Tyree and Richter 1981; Schulte and Hinckley 1985). To calculate C, first Ψ_{tlp} was estimated from the inflection point of the Ψ_L –RWC relationship. The slope of the relationship before turgor loss was multiplied by the saturated water content (mol H_2O) of the shoot and divided (normalized) by total leaf surface area (A_L) (Brodribb et al. 2005). To quantify the maximum amount of foliar water storage, bulk shoot succulence (S, g H_2O m^{-2}) was calculated, which is defined as $(M_F - M_D) / A_L$, where M_D is dry mass (g) of the foliated shoot (Bacelar et al. 2004). C represents the ability of shoots to store water relative to transpiring leaf area, while S represents the maximum amount of water that can be stored. In the process of calculating C, the bulk tissue elastic

modulus was also calculated. Because C is standardized by leaf area, it provides an adequate relative measure of cell wall elasticity.

2.3.4 Leaf morphology and anatomy

To quantify shoot silhouette area (A_S), sample shoots were scanned at 600 dpi using a flatbed scanner (Expression 10000XL, Epson America Inc., Long Beach, CA, USA). All leaves were then removed from the shoot axis, placed on the scanner with no overlap and scanned to quantify projected leaf area (A_P). To observe leaf anatomy, second-year leaves were fixed in FPA, transversely sectioned at mid-point to 20 μm thickness using a microtome and double stained with safranin and fast green. Photographed images (400× magnification) of the transverse leaf sections were used for anatomical analyses. All shoot samples were oven-dried at 70 °C to constant weight to determine M_D.

2.3.5 Data analyses

Hemispherical photographs were analyzed using Gap Light Analyzer (ver 3.1, Simon Frazer University, Bernaby, BC, Canada) to calculate canopy openness, total radiation simulated over a 12-month growing season and three site factors expressing the percentage of direct, indirect and total radiation received. Total site factor (hereafter TSF) was most strongly correlated with hydraulic and morphological variables and therefore used as the measure of light availability. Scanned images of shoots and leaves were analyzed using Image J (National Institutes of Health, Bethesda, USA) to determine A_S and A_P. Leaf mass per area (LMA, g m $^{-2}$) was calculated as the ratio of leaf dry mass to A_P and shoot mass per area (SMA, g m $^{-2}$) as the ratio of M_D to A_S. Perimeter-to-width ratios of leaf transverse sections were multiplied by A_P to obtain A_L (Barclay and

Goodman 2000), which was then used to calculate *C*. All hydraulic and morphological variables were regressed against height and TSF using model fitting in JMP 10 (SAS Institute Inc.). The difference between sites was examined via analysis of covariance (separate slopes model) with height and TSF as covariates.

Table 2.1 Structural attributes of tall *S. sempervirens* trees measured in northern rain forest (Prairie Creek Redwoods State Park) and much drier, southern forest (Landels-Hill Big Creek Reserve) in California, USA. Numbers in parenthesis indicate heights of trunk diameter measurements.

Site / Tree	Height (m)	Diameter (m)
Prairie Creek		
1	109.88	3.42 (6.65)
2	103.95	3.43 (1.55)
3	101.87	6.74 (1.40)
Landels-Hill		
4	79.76	2.18 (2.60)
5	72.91	1.87 (2.30)
6	70.00	2.13 (1.70)

2.4 Results

2.4.1 Leaf water relations

Both hydraulic capacitance (C) and leaf succulence (S) of foliated shoots increased with height (Fig. 2.1a,c, $C = (0.115 \pm 0.062) + (0.00816 \pm 0.00096)\ h$, $P < 0.00001$; $S = (67.7 \pm 9.1) + (1.36 \pm 0.14)\ h$, $P < 0.00001$, where h equals height, $n = 39$). At the same height, both C and S were greater for southern than northern trees (ANCOVA, $F = 12.69$, $P = 0.0011$ and $F = 8.93$, $P = 0.0051$, respectively). However, in relation to total site factor (TSF), there was no distinction between sites (Fig. 2.1b,d, $C = (0.139 \pm 0.028)\ TSF^{(0.434 \pm 0.051)}$, $P < 0.00001$; $S = (63.0 \pm 7.3)\ TSF^{(0.260 \pm 0.031)}$, $P < 0.00001$, $n = 39$). Thus, despite their lower stature (70–80 m), the highest, most exposed leaves of the southern trees had similar water storage capacity as those of the northern trees (>100 m).

In contrast, osmotic potential at turgor loss (Ψ_{tlp}) did not change with height (Fig. 2.2a, $\Psi_{tlp} = -1.972 \pm 0.038$, $P = 0.800$, $n = 39$). Treetop shoots had greater water storage and consequently higher water content at saturation compared to those lower in the crown. This added buffer resulted in lower relative water content at turgor loss (RWC_{tlp}) such that treetop shoots did not lose turgor until they had lost nearly 20% of their saturated water content (Fig. 2.2b, $RWC_{tlp} = (0.878 \pm 0.009) + (-0.00061 \pm 0.00014)\ h$, $P = 0.00001$, $n = 39$).

2.4.2 Leaf morphology and anatomy

Vertical changes in leaf and shoot morphology (LMA and SMA, respectively) closely paralleled those of water storage (Fig. 2.3). In the northern trees, shoot morphology did not change below *c*. 60 m, where light availability was consistently low (6.1 ± 1.2% TSF, $n = 7$), resulting in a nonlinear response. We also found anatomical changes reflecting adaptation for water storage. Transverse-sectional area of transfusion tissue (A_T)

increased, whereas area of xylem tissue (A_X) decreased with height (Fig. 2.4a,b, A_T = $(3.40\times10^{-3}\pm1.53\times10^{-3}) + (1.40\times10^{-4}\pm2.35\times10^{-5})\ h$, $P < 0.0001$; $A_X = (2.06\times10^{-3}\pm 1.16\ \times10^{-4}) - (1.10\times10^{-5}\pm1.77\times10^{-6})\ h$, $P < 0.0001$, $n = 38$). The decrease in A_X with height was attributable to a decrease in the number of xylem tracheids (N_T) (Fig. 2.4c, $N_T = (38.51\pm1.93) - (0.210\pm0.030)\ h$, $P < 0.0001$, $n = 38$) as transverse-sectional area of individual xylem tracheids (a_T) did not change with height (Fig. 2.4d, $a_T = (54.04 \pm2.48) + (0.018\pm0.038)\ h$, $P = 0.644$, $n = 38$).

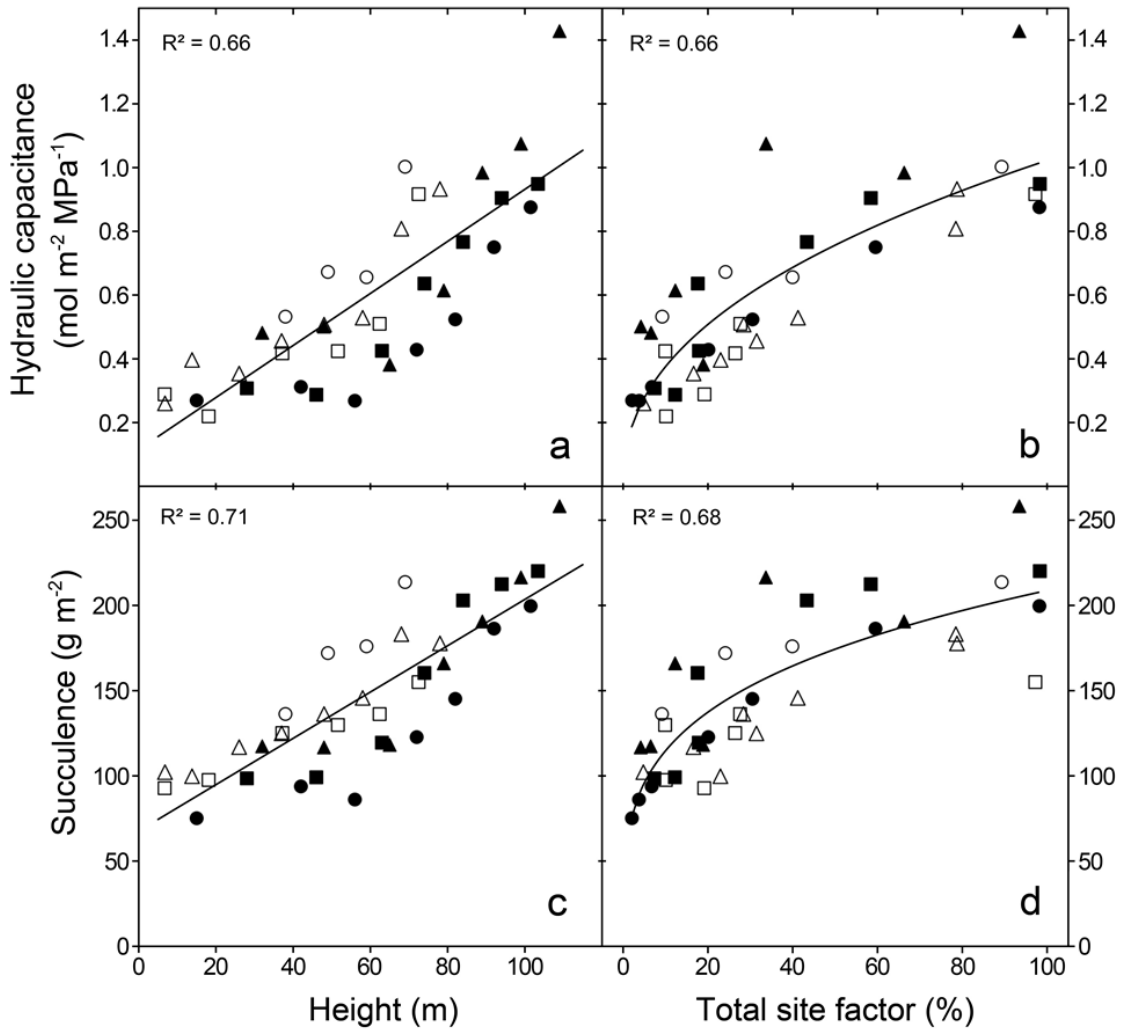

Figure 2.1 Water storage of small, foliated shoots of tall *S. sempervirens* trees. Hydraulic capacitance (**a, b**) and succulence (saturated water content per leaf surface area (**c, d**) shown in relation to height and light availability (total site factor). Each datum represents mean of three to five foliated shoots sampled at each height. Filled and open symbols denote trees in Prairie Creek Redwoods State Park and Landels-Hill Big Creek Reserve, respectively. Symbol shapes denote different trees. Regression lines fitted to data from all six trees.

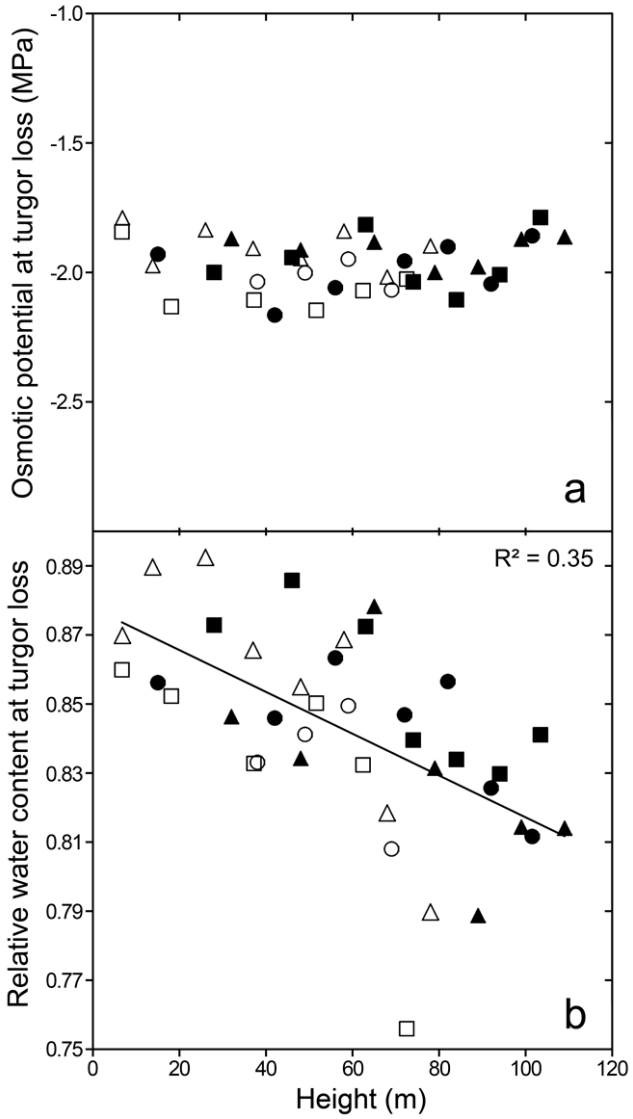

Figure 2.2 Hydraulic properties of foliated shoots of tall *S. sempervirens* trees. Osmotic potential at turgor loss (**a**) and relative water content at turgor loss (**b**) shown in relation to height. Symbols and regression line as in Fig. 1.

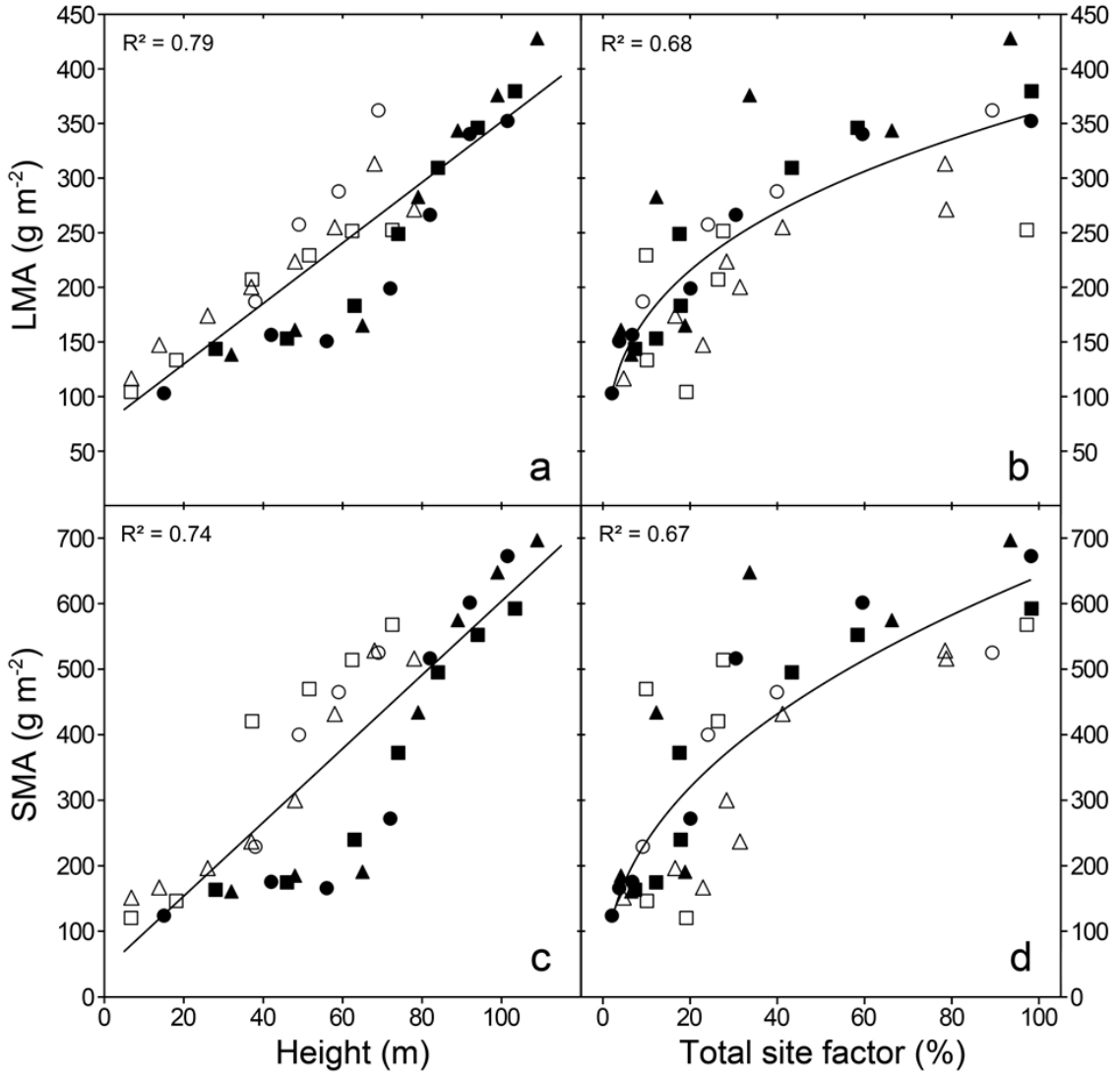

Figure 2.3 Shoot/leaf morphology of tall *S. sempervirens* trees. Leaf mass per area (LMA; **a**, **b**) and shoot mass per area (SMA; **c**, **d**) shown in relation to height and light availability (total site factor). Symbols and regression line as in Fig. 1.

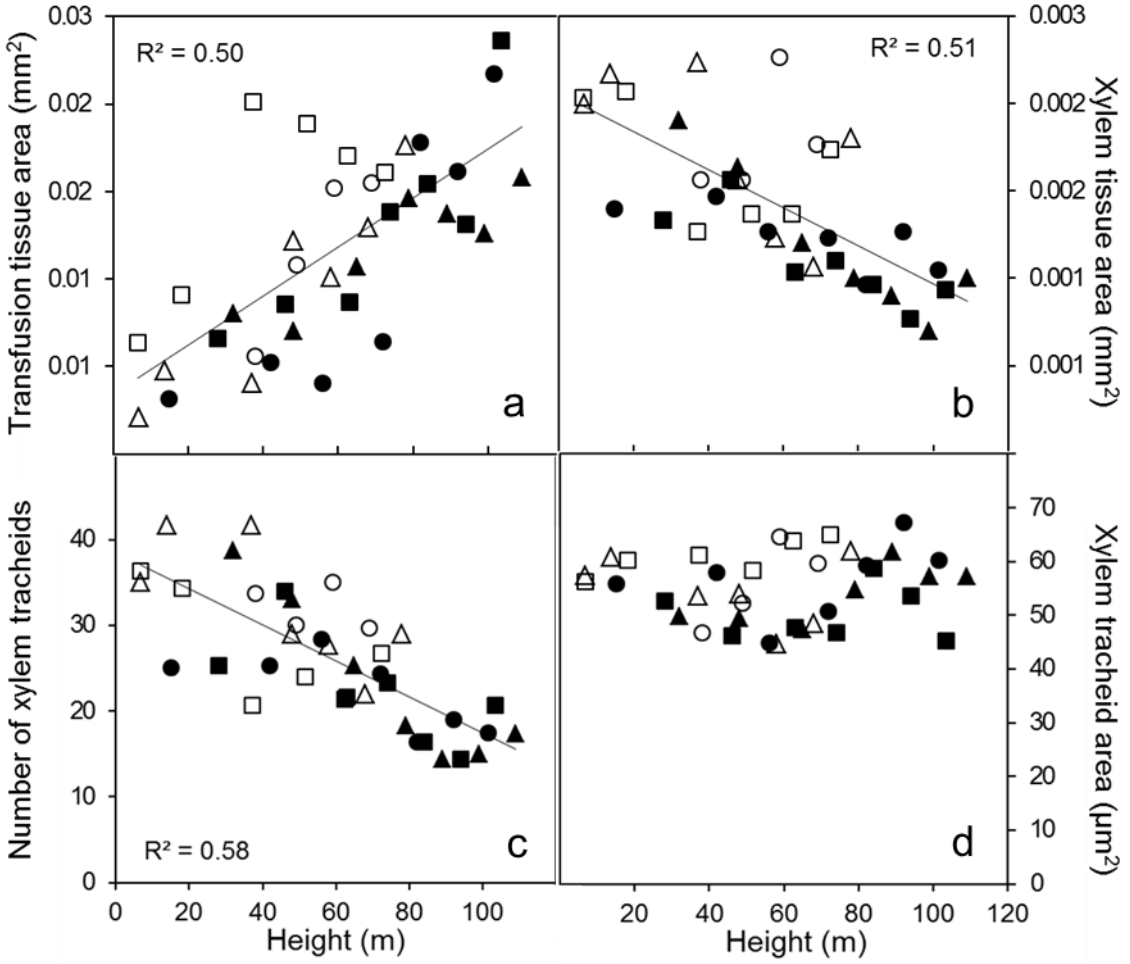

Figure 2.4 Leaf anatomy of tall *S. sempervirens* trees. Transverse-sectional area of transfusion tissue (**a**) and of xylem (**b**), number of tracheids (**c**) and transverse-sectional area of individual tracheids (**d**) shown in relation to height. Symbols and regression line as in Fig. 1.

2.5 Discussion

The structure and orientation of well-illuminated *S. sempervirens* leaves allow them to collect moisture (Fig. 2.5) and absorb it (Burgess and Dawson 2004; Simonin, Santiago and Dawson 2009). The results demonstrate that some of this water can be stored internally, which could reduce reliance on water transport from roots. Foliar water uptake and storage have positive effects on physiological function in water-stressed plants (e.g. Martin and Willert 2000; Breshears et al. 2008). The ability of *S. sempervirens* foliage to store water increases with both height and light availability such that treetop shoots have maximum hydraulic capacitance and succulence. Compared to those lower in the crown, treetop shoots experience greater hydrostatic and hydrodynamic constraints on their internal water supply. Foliar water storage helps explain why, despite being the tallest species, midday xylem pressures in treetop shoots of *S. sempervirens* are not as low as in other tall species (Koch et al. 2004; Ishii et al. 2008), which tolerate increasing water stress with height by reaching lower daytime water potentials and turgor loss points (Bauerle et al. 1999; Woodruff, Bond and Meinzer 2004). Foliar water storage is also consistent with the occurrence of xylem flow reversal in treetop branches of *S. sempervirens* (Burgess and Dawson 2004).

The mean daytime transpiration rate documented for *S. sempervirens* treetops (*c*. 0.06 mmol H_2O m^{-2} s^{-1}; Ambrose et al. 2010) multiplied over a 10-h daytime period amounts to 38.9 g H_2O m^{-2}. Thus, given the mean succulence documented here for treetop shoots (204.1 g H_2O m^{-2}), foliage alone can store more than five times the daily transpirational demand at the treetop. Because effects of the gravitational potential gradient were removed in our cut-rehydrate treatment, and foliage under chronic water stress cannot remain fully saturated in situ, our succulence calculations likely represent maximum

values for foliar water storage. Nevertheless, the magnitude of foliar water storage may help treetop leaves avoid turgor loss, maintain stomatal functioning and sustain photosynthesis.

Plant leaves under increasing water stress often acclimate by lowering the turgor loss point (Pallardy 2007). In tall trees of *P. menziesii*, Ψ_{tlp} decreases with increasing height (Bauerle et al. 1999; Woodruff, Bond and Meinzer 2004). In this study, it was found that increasing succulence and decreasing RWC_{tlp} contributed to maintaining Ψ_{tlp} constant within the crown of tall *S. sempervirens* trees. This mechanism is similar to succulent plants that utilize stored water in dry habitats (Zimmermann and Milburn 1982; Barcikowski and Nobel 1984). The observations of xylem pressure responses to excess water during pressure–volume measurements imply that when water potential decreases, stored water can be used to prevent xylem pressures from dropping further. Independent analyses of *S. sempervirens* leaf anatomy revealed that transfusion tissue surrounding the xylem may collapse during periods of high water stress, such that water stored therein can enter xylem tracheids and provide a leaf-level hydraulic buffer against cavitation (Oldham et al. 2010). Increasing area of transfusion tissue relative to xylem suggests increasing dependence on stored water and decreasing reliance on water transport with increasing height.

In many gymnosperms, there appears to be a trade-off between xylem safety and vulnerability to cavitation such that tracheid diameters in the main stem and branches decrease with increasing height (Hacke and Sperry 2001; Tyree and Zimmermann 2002; Sperry, Meinzer and McCulloh 2008). In tall *P. menziesii* trees, both the quantity and diameter of leaf tracheids decrease with increasing height (Woodruff, Meinzer and Lachenbruch 2008). In contrast, leaf tracheid diameter was constant with respect to height

in tall *S. sempervirens*. The safety margin against cavitation may be larger for stem and branches as opposed to leaves because loss of function in the former would lead to more extensive damage. Recent theoretical work suggests that xylem tapering cannot compensate completely for the hydraulic limitations of tree growth (Zaehle 2005), leaving open the possibility that other compensating mechanisms are involved. The results of this study indicate that anatomical changes may help maintain homeostasis of shoot hydraulic functioning in *S. sempervirens*. In the upper crown, leaves fuse to the shoot axis creating a relatively large tissue volume and intercellular space surrounding xylem that likely stores more water per unit xylem than in the lower crown (Fig. 2.6). In addition to quantitative aspects of leaf and shoot anatomy, decreasing RWC_{tlp} and increasing hydraulic capacitance with increasing height and light availability reflect greater cell-wall elasticity, which enhances the potential of individual cells, including transfusion tissue, to expand and store water (Brodribb et al. 2005).

Similar leaf- and shoot-level responses to light availability in taller northern and shorter southern forests suggest that on top of the hydrostatic gradient, which increases linearly with height, evaporative demand driven by light intensity helps determine morphological, anatomical and physiological characteristics of *S. sempervirens* foliage. Associated with height- and light-related changes in shoot structure, various hydraulic resistances within leaves also limit photosynthesis (Sack and Holbrook 2006; Brodribb, Field and Jordan 2007; Mullin et al. 2009). In *S. sempervirens*, water storage near the site of photosynthesis helps overcome these constraints, explaining how the world's tallest species solves the dilemma that water stress is greatest where light availability for photosynthesis is highest.

Figure 2.5 Treetop leaves of the tallest *S. sempervirens* (115.72 m in 2012 when photograph was taken) still retain dew droplets on leaf surfaces by mid-morning. Scale on right indicates 6 cm of vertical growth since 2011.

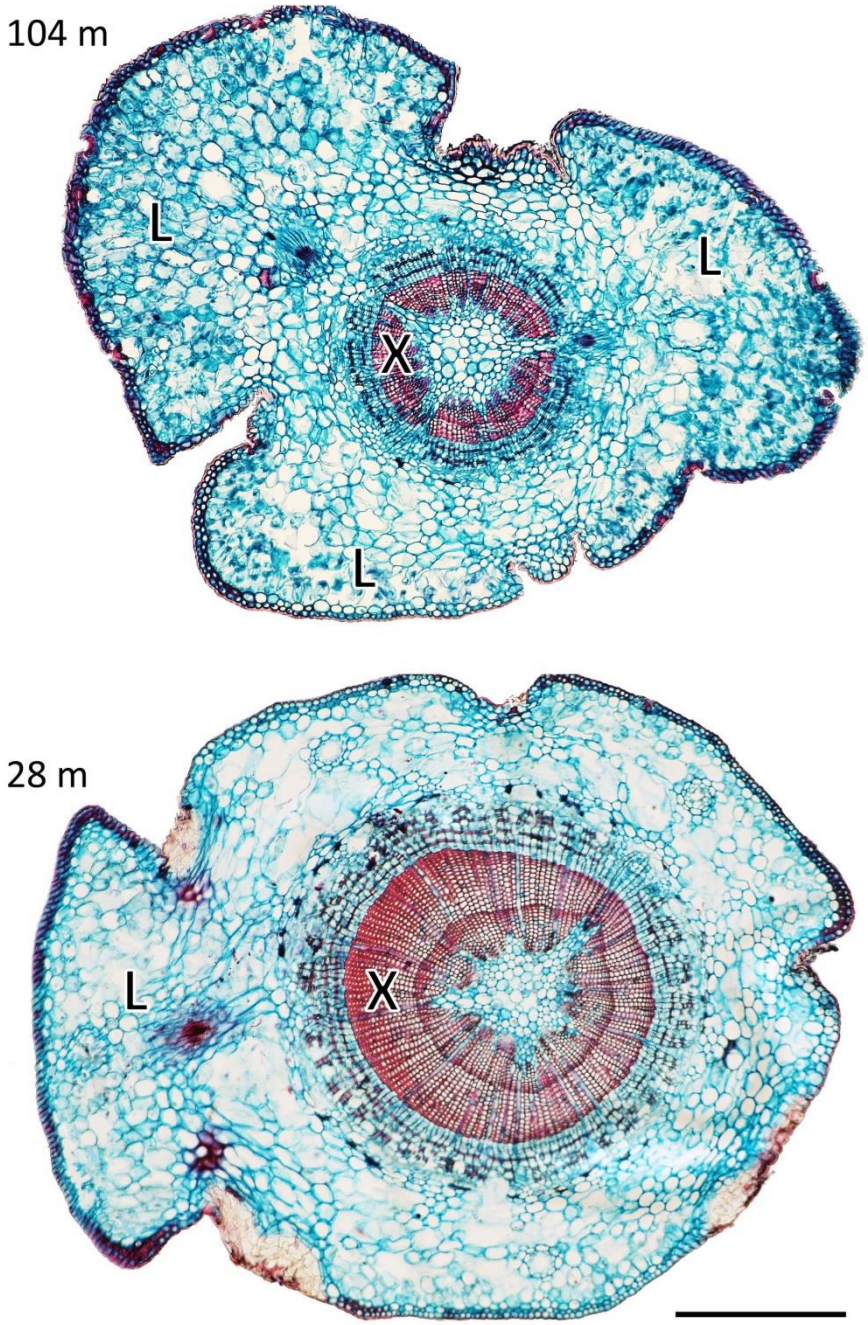

Figure 2.6 Transverse-sectional anatomy of second-year foliated shoots at 104 m (top) and 28 m (bottom) in a 110-m-tall *S. sempervirens* tree. Relative area of xylem (X: stained red at center with two annual rings) is smaller in treetop shoots whose fused stem and leaf parenchyma (L) create relatively large volume for potential water storage surrounding central conducting tissues. In contrast, leaves in lower-crown shoot are separated from stem and only leaf base is attached on left side of stem. Scale bar = 500 μm.

Chapter 3

Function and structure of leaves contributing to increasing water storage with height in the tallest *Cryptomeria japonica* trees of Japan

3.1 Abstract

The tallest trees of *Cryptomeria japonica* occur in climatic regions similar to the world's tallest trees. Thus it can be hypothesized that tall *C. japonica* trees would have evolved adaptive mechanisms to overcome height growth limitation. This study focused on foliar water storage, a mechanism recently discovered in *Sequoia sempervirens*. In *C. japonica*, leaf water potential (osmotic potential in Chapter1) at turgor loss did not change with height or light availability, while leaf hydraulic capacitance and succulence (water content per leaf surface area) increased, suggesting hydraulic compensation. Plasticity of leaf morphology could contribute to avoiding negative effects of height on photosynthesis. This study also focused on the structure and function of transfusion tissue in leaves and its role in water storage and supply. Cross-sectional area of transfusion tissue increased with height, whereas that of xylem was constant. It was confirmed that water flowed from vascular bundle to mesophyll via the transfusion tissue. Cryo-scanning electron microscopy images of leaf cross sections showed that transfusion cells were flattened, but not fully dehydrated when leaf water potential decreased in situ and by experimental dehydration, and cell deformation was more marked for treetop leaves than for lower-crown leaves. The shape of transfusion cells recovered at predawn as well as after experimental rehydration. As in *S. sempervirens*, transfusion tissue of *C. japonica* may function as a hydraulic buffer, absorbing and releasing water according to leaf water status. Anatomical and hydraulic properties contributing to foliar water storage may be an adaptive mechanism acquired by tall Cupressaceae trees to overcome the hydraulic constraints on physiological function with increasing height.

3.2 Introduction

The hydraulic limitation hypothesis (HLH, Ryan and Yoder 1997) proposed that as tree height increases, available water decreases due to increasing hydrostatic pressure and distance of water transport, while water demand for transpiration and photosynthesis increases (Cowan 1982; Zimmermann 1983; Midgley 2003). The resulting water stress constrains various physiological processes such as photosynthetic production (Ambrose et al. 2010), turgor needed for cell expansion (Woodruff et al. 2004), etc., ultimately limiting height growth (Ryan et al. 2006). However, HLH alone cannot explain growth decline with increasing height (McDowell et al. 2002; Niinemets 2002). Hydraulic limitation could be compensated in various ways, including decreasing leaf water potential (Barnard and Ryan 2003), osmotic adjustment (Woodruff et al. 2004) and water storage (Phillips et al. 2003; Scholz et al. 2011). While height growth of normal-statured trees may indeed be hydraulically limited (e.g., Nabeshima and Hiura 2008; Renninger et al. 2009; Meinzer et al. 2010), the prominent tall trees are likely to have evolved adaptive mechanisms to overcome hydraulic limitation (Chapter 2), which would explain why they grow so much taller than other species. In tall and large trees of the world, growth rates continue to increase with increasing tree size (Ambrose et al. 2010; Stephenson et al. 2014; Sillett et al. 2015) suggesting that, despite their great size, these trees are not carbon limited as HLH would predict.

The hydraulic limitation hypothesis is also based on the assumption that the only source of water for trees is from the roots. However, in *Sequoia sempervirens*, the tallest species, absorption of moisture from leaf surfaces and water storage in leaves alleviates water stress in treetop leaves decoupling leaf water status from soil moisture content and decreasing reliance on long-distance water transport from roots (Chapter 2; Burgess and

Dawson 2004; Simonin et al. 2009). In *S. sempervirens*, as show in Chapter 2, hydraulic capacitance and succulence of leaves increase with height, and tree top leaves have capacity to store more than five times the daily transpiration demand. As a result, despite decreasing leaf water potential with increasing height (Koch et al. 2004; Ishii et al. 2008), leaf osmotic potential at turgor loss, which is expected to decrease when leaves experience constant drought conditions (Pallardy 2007; Rodriguez et al. 2012; Negret et al. 2013), remains constant within the crown of *S. sempervirens* (Chapter 2). Although these results indicate the importance of foliar water storage for maintaining the water status of treetop leaves in tall trees, the detailed hydraulic mechanism and anatomical features involved are not fully understood.

This study focused on anatomical features of leaves that could contribute to foliar water storage. As part of the hydraulic system in addition to the xylem, transfusion tissue, specific to gymnosperms and composed of tracheids and parenchyma cells, is suggested to function as a pipeline for water and nutrients between the vascular bundle and leaf mesophyll (Takeda 1931; Hu and Yao 1981; Brodribb et al. 2010; Aloni et al. 2013). In some gymnosperms, transfusion cells lacking endodermis or bundle sheath collapse easily under experimentally induced negative pressure (Brodribb and Holbrook 2005; Zhang et al. 2014). This is associated with declines in leaf hydraulic conductance (K_{leaf}), but is easily reversible (Zhang et al. 2014) . In *S. sempervirens*, transverse-sectional area of transfusion tissue increases with height (Chapter 2) and collapsed transfusion cells were observed close to vascular cells in the upper-crown leaves suggesting (Oldham et al. 2010). These observations suggest transfusion tissue serves to protect the xylem from embolism by releasing stored water, temporarily relieving tension in the xylem, which could compensate negative effects of hydraulic limitation with increasing height.

However, there are no investigations of the hydraulic function of transfusion tissue in tall trees.

The world's tallest trees appear to grow in thermally similar climates (Larjavaara 2014). The tallest trees in Japan, *Cryptomeria japonica* (Cupressaceae), are found in the northwest coast of Honshu Island in humid continental climate, which is a localized temperate, maritime climate similar to Mediterranean and maritime west coast climates (climate classification according to Peel et al. 2007), where the tallest gymnosperm (*S. sempervirens*) and angiosperm (*Eucalyptus regnans*) occur, respectively. *C. japonica* is also the major plantation tree in Japan and a valuable forest resource. Because *C. japonica* and *S. sempervirens* belong to the same family and grow tall in similar climates, it could be hypothesized that the tallest *C. japonica* trees would have evolved adaptive mechanisms to overcome hydraulic limitation, similar to *S. sempervirens*. To test this, vertical changes in leaf hydraulic properties were investigated focusing on foliar water storage, the compensating mechanism discovered in *S. sempervirens* described in Chapter 2. leaf anatomy was also observed both in situ and in the laboratory to elucidate the role of transfusion tissue in leaf hydraulic functioning.

3.3 Materials and methods

3.3.1 Study site

The study was conducted at Nibuna-Mizusawa Forest Reserve (NMFR), Tashirozawa National Forest in Akita Prefecture, Japan (40.08 °N, 140.25 °E, and 200 m ASL). The site is a mixed forest composed of ca. 250 year-old *C. japonica* trees and deciduous broadleaved trees, such as *Aesculus turbinata* and *Pterocarya rhoifolia*. The NMFR was designated to protect the tallest *C. japonica* forest in Japan. Tree height and diameter at breast height (DBH, 1.3 m above ground level) of the 159 *C. japonica* trees in the 1-ha research plot established by Akita Pref. Univ. were, 49.8 ± 1.8 m and 111.6 ± 5.5 cm (mean ± SD), respectively in 2012. Mean annual precipitation is 1671.1 mm and mean annual temperature is 10.2 °C in 1981−2010. Snow covers the ground from early December to late March and maximum snow depth in 2013 was 131 cm.

3.3.2 Foliage sampling and measurement of light environment

In May 2013, single-rope climbing technique was used for accessing the crown of four study trees (Table 3.1) and stretched a tape measure from treetop to ground level. small branches (30−50 cm long) with attached foliage were collected from the outer crown of each tree at 5−10 m intervals from just below treetop to the lowest living branches in the four trees (height range 19−52 m).

Hemispherical photographs were taken directly above each sampling location and calculated light availability expressed as canopy openness (%) using Gap Light Analyzer (ver 3.1, Simon Frazer University, Bernaby, BC, Canada). The sampled branches were immediately re-cut under water, sealed in black plastic bags, and fully rehydrated in the laboratory overnight.

3.3.3 Leaf water relations

The pressure-volume curve of three small, foliated shoots from each sampled branch comprising second- and current-year internodes, were obtained using the bench-drying approach to the pressure-volume technique (Tyree and Hammel 1972; Schulte and Hinckley 1985). Bulk leaf water potential (Ψ_L, MPa) was measured repeatedly with a pressure chamber (Model 1000, PMS Instruments, Corvallis, USA) and fresh weight of the sample shoots before and after each water potential reading. Care was taken to increase and decrease the pressure in the chamber very slowly (less than 0.01 MPa s^{-1}) so as not to damage the sample shoots (repeat pressurization method, Hinckley et al. 1980; Ritchie and Roden 1985; Parker and Colombo 1995).

After the pressure-volume measurement, all the sample shoots were photographed for measurement of total leaf surface area (A_L, m^2) as described below, and then oven-dried to constant weight to obtain leaf dry mass (M_D, g). The following variables were calculated to estimate drought tolerance of shoots: fresh weight at saturation (M_F, g), osmotic potential at saturation (Ψ_{sat}, MPa), osmotic potential at turgor loss (Ψ_{tlp}, MPa), relative water content at turgor loss (RWC_{tlp}) at the bulk shoot level. Ψ_{tlp} is a physiological measure of plant water stress (Bartlett et al. 2012), which decreases if leaves experience constant drought conditions (e.g., Pallardy 2007; Rodriguez et al. 2012; Negret et al. 2013).The saturated leaf water content ($M_W = M_F - M_D$) was used for calculating leaf hydraulic capacitance (C_L, mol m^{-2} MPa^{-1}), and succulence (S_L, g H_2O m^{-2}).

$$C_L = \delta RWC / \delta \Psi_L \, (M_D / A_L) \, (M_W / M_D) / M$$

$$S_L = M_W / A_L$$

where, $\delta RWC / \delta \Psi_L$ is the slope of the ΨL-RWC relationship calculated from the pressure-volume curve and M is the molecular weight of water.

3.3.4 Leaf morphology and anatomy

After pressure-volume measurement, each sample shoot was placed on a slide-viewer, illuminated from below, and photographed to obtain the shoot silhouette image. Then all leaves were detached from the shoot axis, laid on the slide viewer without overlap, and photographed. Photographed images of shoots and leaves were analyzed using image analysis software (Image-J ver. 1.48; National Institute of Health, USA) to quantify shoot silhouette area (A_S, m^2) and projected leaf area (A_P, m^2). To obtain A_L, perimeter-to-width ratios obtained from leaf transverse sections were multiplied by A_P (Barclay and Goodman 2000). These measurements were used to calculate leaf mass per area (LMA = M_D / A_P, g m-2) and shoot silhouette area to projected leaf area ratio (SPAR = A_S / A_P), a measure of leaf overlap within the shoot.

Second-year leaves of a different set of sample shoots from the same branches were fixed with FAA (formalin, acetic acid, 50% ethyl alcohol; 5:5:90 v/v) and washed under tap water overnight. For all heights, transverse sections (24μm thickness) were taken consistently from the same part of the leaf (at the midpoint between leaf tip and its attachment to the stem) using a sliding microtome installed with a holder for frozen sectioning (REM-710, Yamato Kohki Industrial Co., LTD., Japan). Leaf sections were double stained with safranin-fast green to differentiate lignified cells and living cells. Three leaf transverse sections from each sampled branch were observed under an optical microscope (Nikon, Eclipse 80i, Nikon, Tokyo) and photographed with a digital camera (E-620, Olympus, Tokyo). Then, we quantified the cross-sectional area of xylem (A_X, mm^2) and transfusion tissue (A_{TT}, mm^2) using Image-J.

3.3.5 Structure and function of transfusion tissue

To roughly detect the pathway of water flow through leaf tissues, the cut end of foliated shoots comprising third-, second- and current-year internodes sampled from 50 and 26 m height were immersed in an aqueous solution of 0.5% (w/v) acid fuchsin. After 1 and 2 hours, we observed by eye that the leaf apices were stained red indicating that the shoots had absorbed the acid fuchsin. Three leaves from each shoot were transversely sectioned at midpoint to 24 μm thickness using same methods as described above. The leaf sections were observed under the optical microscope.

To observe diurnal changes in leaf anatomy and water status, intact foliated shoots at treetop (52 m and 51 m) and lowest (26 m and 19 m) branches in two of the study trees were flash-frozen in situ in liquid nitrogen (LN_2) at predawn and midday on a clear day in September 2014. The frozen shoots were then cut and kept immersed in LN_2, transported to the laboratory, and stored in a freezer at –80 °C. A fresh transverse surface was made at the midpoint of second-year leaves from each frozen shoot using an electronic microtome cryostat (HM 505 E, Microm International, Walldorf, Germany) at –35 °C. The specimen was attached to the holder with Tissue-Tek Embedding Compound (Sakura FinetekUSA, Torrance, CA, USA), and then transferred to a cryo-scanning electron microscopy system (cryo-SEM; JSM6510, JEOL, Tokyo, Japan). Secondary electron images were obtained at an accelerating voltage of 3kV with shallow sublimation to observe water within the leaf structure. After obtaining images, samples were sublimated deeply for approximately 30 min to remove water from the sample surfaces to observe the leaf structure clearly.

Along with the frozen samples, a pair of small branches (30−50 cm long) was collected from each of the sampling locations at midday. Using one set of these samples, bulk leaf

water potential (Ψ_L) was measured with a pressure chamber as reference of in situ Ψ_L at midday. The remaining set of sample branches were immediately re-cut under water, sealed in black plastic bags, and fully rehydrated in the laboratory overnight. Three to five foliated shoots on the rehydrated branches were flash-frozen in LN_2 before removal from the branch. Three to five additional shoots were bench-dried until Ψ_L reached values similar to that at midday in the field, then flash-frozen in LN_2. Cryo-SEM images of the rehydrated and bench-dried leaves before and after deep sublimation were obtained using the same methods as described above.

The cryo-SEM images were analyzed to compare the shape of transfusion cells under different conditions. In each image, ten transfusion cells were randomly chosen and measured cross-sectional area (A_{TC}, μm^2) and perimeter (P_{TC}, μm) using Image J to calculate circularity ($C_{TC} = 4\pi A_{TC} / P_{TC}^2$) of each transfusion cell.

3.3.6 Statistical analyses

For each variable of leaf water relations, leaf morphology and leaf anatomy, intercepts and slopes of the relationships among study trees were compared by analysis of covariance (ANCOVA) with individual study trees as the random effect and height and canopy openness as the covariate. Although the random effect of the study trees was significant for some variables, the relationships with height and canopy openness was similar for all study trees. Thus in order to examine species characteristics, we pooled the data for all study trees and analyzed each variable in relation to height and canopy openness using regressions analysis.

A_{TC} and C_{TC} between different water statuses and heights were compared by three-way analysis of variance (ANOVA) with water status and height as the main effects and study

trees as a random effect. Although the random effect of the study tree was marginally significant ($F > 4.8$, $P < 0.048$) for some variables, the trends were similar for all study trees. All statistical analyses were done using JMP 11 (SAS Inc., Cary, NC, USA).

Table 3.1 Structural attributes of four *C. japonica* study trees at NMFR.

Tree	Height (m)	Diameter at breast height (m)
1	51.5	114.0
2	50.1	105.3
3	48.7	117.9
4	47.8	109.2

3.4 Results

3.4.1 Leaf water relations

Osmotic potential at turgor loss (Ψ_{tlp}) did not change with either height or canopy openness (Figs 3.1a and 3.1b; $P = 0.89$ and $P = 0.23$, respectively). Osmotic potential at saturation (Ψ_{sat}) did not change with height or canopy openness (Figs 3.1c and 3.1d; $P = 0.39$ and $P = 0.54$, respectively). Relative water content at turgor loss (RWC_{tlp}) increased with both height and canopy openness ($R^2 = 0.18$, $P = 0.002$ and $R^2 = 0.18$, $P = 0.002$, respectively). Leaf hydraulic capacitance (C_L) and succulence (S_L) both increased with height (Figs 3.1e and 3.1g; $P = 0.04$ and $P < 0.0001$, respectively). C_L and S_L of treetop leaves were almost twice that of lower crown leaves. In relation to canopy openness, C_L did not change, while S_L increased consistently (Figs 3.1f and 3.1h; $P = 0.26$ and $P < 0.0001$, respectively).

3.4.2 Leaf morphology and anatomy

Leaf area of the sample shoots was constant within the crown ($R^2 = 0.006$, $P = 0.58$) but leaf dry mass increased with height ($R^2 = 0.21$, $P = 0.0006$). As a result, Leaf mass per area (*LMA*) increased with both height and canopy openness (Figs 3.2a and 3.2b; $P < 0.0001$ and $P < 0.0001$, respectively). Shoot silhouette area to projected leaf area ratio (*SPAR*) decreased with height and canopy openness (Figs 3.2c and 3.2d; $P < 0.0001$ and $P = 0.0004$, respectively), that is to say treetop leaves are arranged spherically along the shoot axis with more overlap than lower-crown leaves.

Cross-sectional area of xylem (A_X) did not change with either height or canopy openness (Figs 3.2e and 2f; $P = 0.58$ and $P = 0.52$, respectively), whereas that of transfusion tissue (A_{TT}) increased with both height and canopy openness (Figs 3.2g and 3.2h; $P < 0.0001$ and $P < 0.0001$, respectively), such that A_{TT} of treetop leaves was three

times that of lower-crown leaves.

3.4.3 Structure and function of transfusion tissue

Transfusion tissue was located on both sides of the vascular bundle surrounded with bundle sheath (Fig. 3.3). One hour after the absorption of acid-fuchsin solution, xylem, phloem and transfusion tissues of both samples at 50 m and 26 m were stained (white arrows in Fig 3.3b). Two hours after the absorption, cells in the mesophyll were also stained (white arrows in Fig 3.3c), indicating that water flowed from xylem to mesophyll via transfusion tissue.

The cryo-SEM images of leaves flash-frozen in situ are shown in Fig 3.4, while the images of leaves flash-frozen in the laboratory are shown in Fig 3.5. The explanation below is common to all observed leaves of the two study trees.

In leaves flash-frozen in situ at predawn, all transfusion cells and xylem tracheids of both the top (Fig 3.4b) and lower-crown leaves (Fig 3.4c) were filled with water and fully expanded. In leaves flash-frozen in situ at midday, all transfusion cells of both the top (Fig 3.4d; $\Psi_L = -18.6$ MPa, for both study trees) and lower-crown (Fig 3.4e; $\Psi_L = -15.5$ and -12.2 MPa, for the two study trees) leaves were filled with water, but some transfusion cells were flattened and/or concave shape (arrows in Fig 3.4d and 3.4e), while xylem cells were filled with water and their shapes were maintained. In all cryo-SEM images of top and lower-crown leaves, xylem embolism was not observed regardless of conditions or treatments. The shapes of bundle sheath and phloem were also maintained (Fig 3.4d and 3.4e). The shape of the deformed transfusion cells was more clearly shown in the cryo-SEM images after deep sublimation (arrows in Fig 3.4f and 3.4g).

In cryo-SEM images of leaves after rehydration in the laboratory, all transfusion cells

and xylem tracheids of both the top (Fig 3.5a) and lower-crown leaves (Fig 3.5b) were filled with water and fully expanded. This was similar to the leaves flash-frozen in situ at predawn (Fig 3.4b and 3.4c). After bench drying to Ψ_L values equal to those observed at midday in the field, however, all transfusion cells of both the top (Fig 3.5c) and lower-crown leaves (Fig 3.5d) were filled with water but some transfusion cells were flattened and/or concave shape (arrows in Fig 3.5c and 3.5d), while xylem cells were filled with water and their shapes were maintained. In all cryo-SEM images of top and lower-crown leaves, xylem embolism was not observed. The shape of bundle sheath and phloem were also maintained (Fig 3.5c and 3.5d). The shape of the deformed transfusion cells was more clearly shown in the cryo-SEM images after deep sublimation (arrows in Fig 3.5e and 3.5f).

In leaves flash-frozen in situ, A_{TC} at midday was smaller than that at predawn for both treetop and lower-crown leaves ($F = 38.1$, $P < 0.001$). C_{TC} at midday was lower (more flattened) than at predawn (Table 3.2, $F = 89.8$, $P < 0.001$) and the difference was greater for treetop leaves than for lower-crown leaves ($F = 12.5$, $P = 0.007$). For both treetop and lower-crown leaves frozen in the laboratory, A_{TC} and C_{TC} of bench-dried leaves were lower and smaller, respectively than that of rehydrated leaves ($F = 20.0$, $P < 0.001$ and $F = 49.6$, $P < 0.001$, respectively).

Table 3.2 Circularity (C_{TC}) and cross-sectional area (A_{TC}) of transfusion cells of treetop and lower-crown leaves of *C. japonica* under various conditions and water statuses

		C_{TC}			A_{TC} (μm^2)		
Condition	Water status	Top	Lower		Top	Lower	
in situ	Predawn	0.79 ± 0.11	0.86 ± 0.08	+	241 ± 127	214 ± 95	
	Midday	0.57 ± 0.10	0.66 ± 0.12	*	94 ± 62	105 ± 75	*
in the laboratory	Rehydration	0.80 ± 0.11	0.83 ± 0.12		184 ± 121	188 ± 79	
	Bench-dried	0.60 ± 0.12	0.67 ± 0.13	*	101 ± 55	106 ± 58	*

Values are the mean (± one s.d.) of ten transfusion cells randomly chosen from each cryo-SEM image. * and + denote significant differences ($P < 0.001$) between water statuses and crown position, respectively.

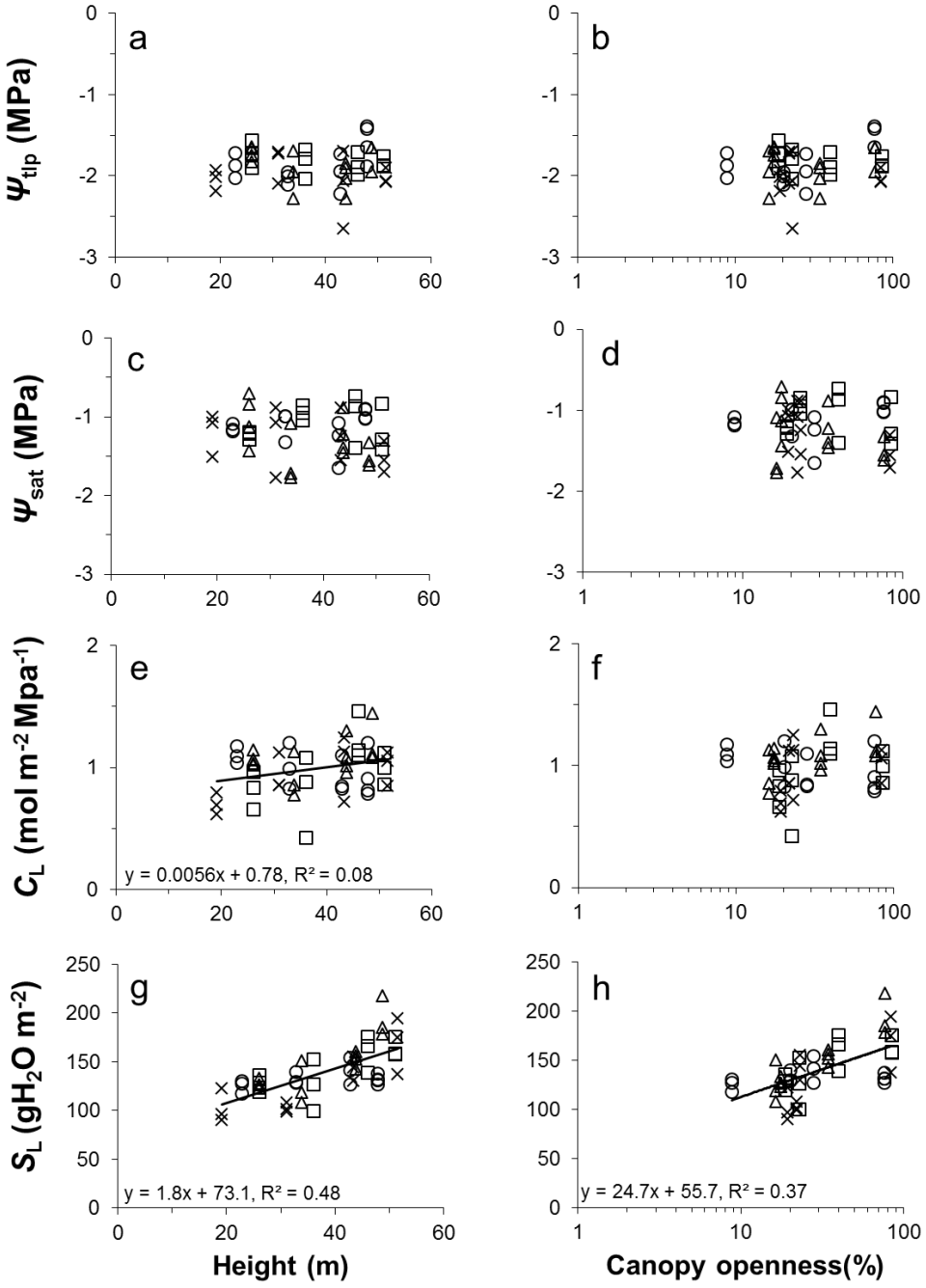

Figure 3.1 Leaf water relations of *Cryptomeria japonica* trees. Osmotic potential at turgor loss (**a**, **b**), osmotic potential at saturation (**c**, **d**), leaf hydraulic capacitance (**e**, **f**), and succulence (**g**, **h**) shown in relation to height and light availability (canopy openness). Lines indicate significant linear regressions ($P < 0.01$, except relationship between C_L and height is $P = 0.04$). Symbol shapes denote different trees.

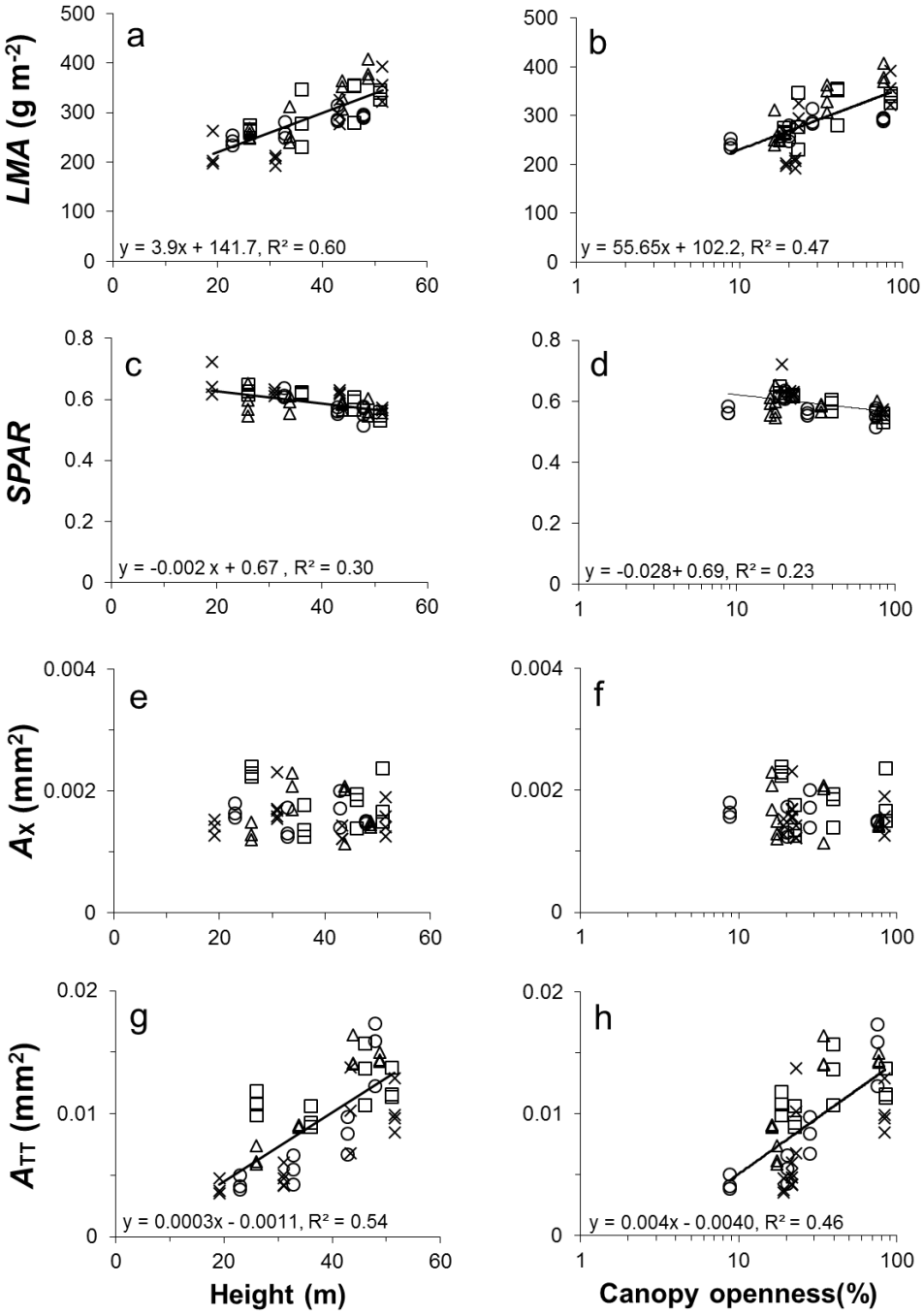

Figure 3.2 Leaf morphology and anatomy of *C. japonica* trees. Leaf mass per area (**a**, **b**), shoot silhouette area to projected leaf area ratio (**c**, **d**), transverse-sectional area of xylem (**e**, **f**), and of transfusion tissue (**g**, **h**) shown in relation to height and light availability (canopy openness). Lines indicate significant linear regressions ($P < 0.01$) and symbols shapes denote different trees.

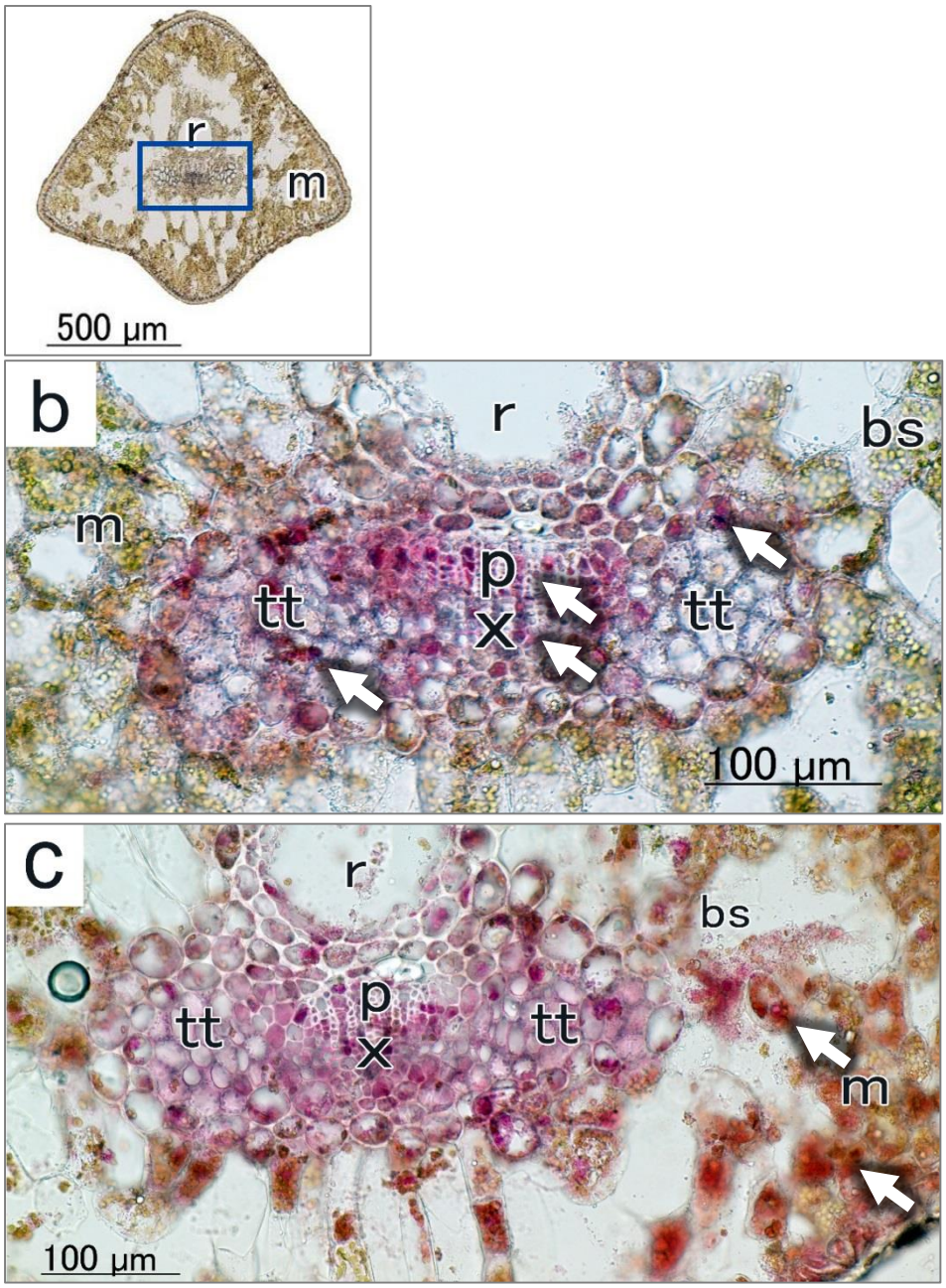

Figure 3.3 (**a**) Transverse-section of a second-year leaf at treetop (50m) of *C. japonica*. (**b**) Closed up of the rectangular region in (**a**), one hour after absorption of acid-fuchsin solution, where phloem, xylem, and transfusion tissue were stained by acid-fuchsin (e.g., *arrows*). (**c**) Two hours after absorption, the mesophyll was also stained (e.g., *arrows*). *Abbreviations* r; resin duct, m; mesophyll, p; phloem, x; xylem, tt; transfusion tissue, bs; bundle sheath.

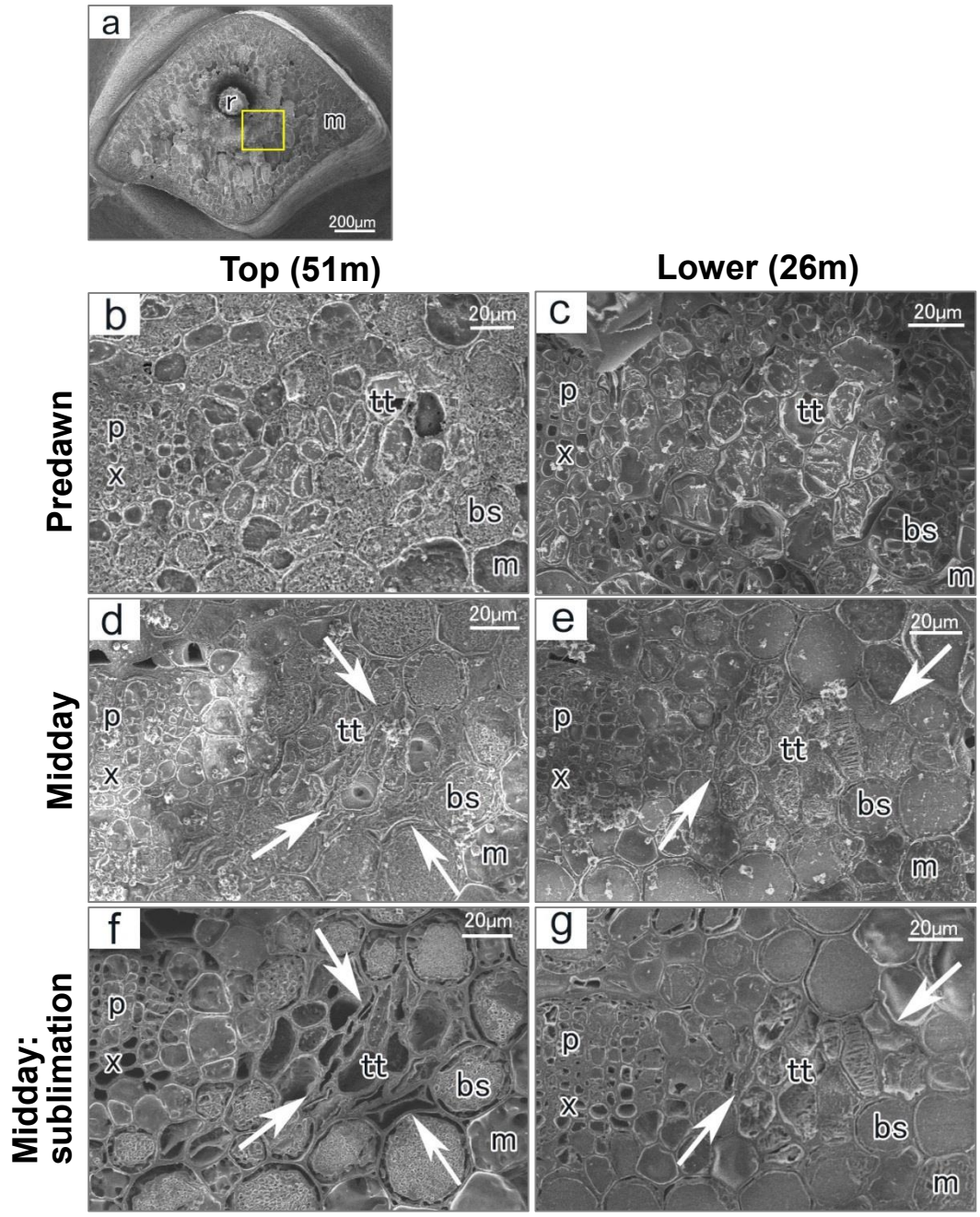

Figure 3.4 (**a**) Cryo-SEM images of transverse-surface of a second-year leaf of *C. japonica*. (**b**)–(**g**) Closed up of the rectangular region in (**a**). Treetop (51 m; **b**, **d**, **f**) and lower-crown (26 m; **c**, **e**, **g**) leaves were flash-frozen in situ at predawn (**b**, **c**) and at midday (**d**, **e**) on a clear day. (**f**) and (**g**) were taken after deep sublimation of (**d**) and (**e**), respectively. *Arrows* denote examples of deformed transfusion cells. *Abbreviations* r; resin duct, m; mesophyll, p; phloem, x; xylem, tt; transfusion tissue, bs; bundle sheath.

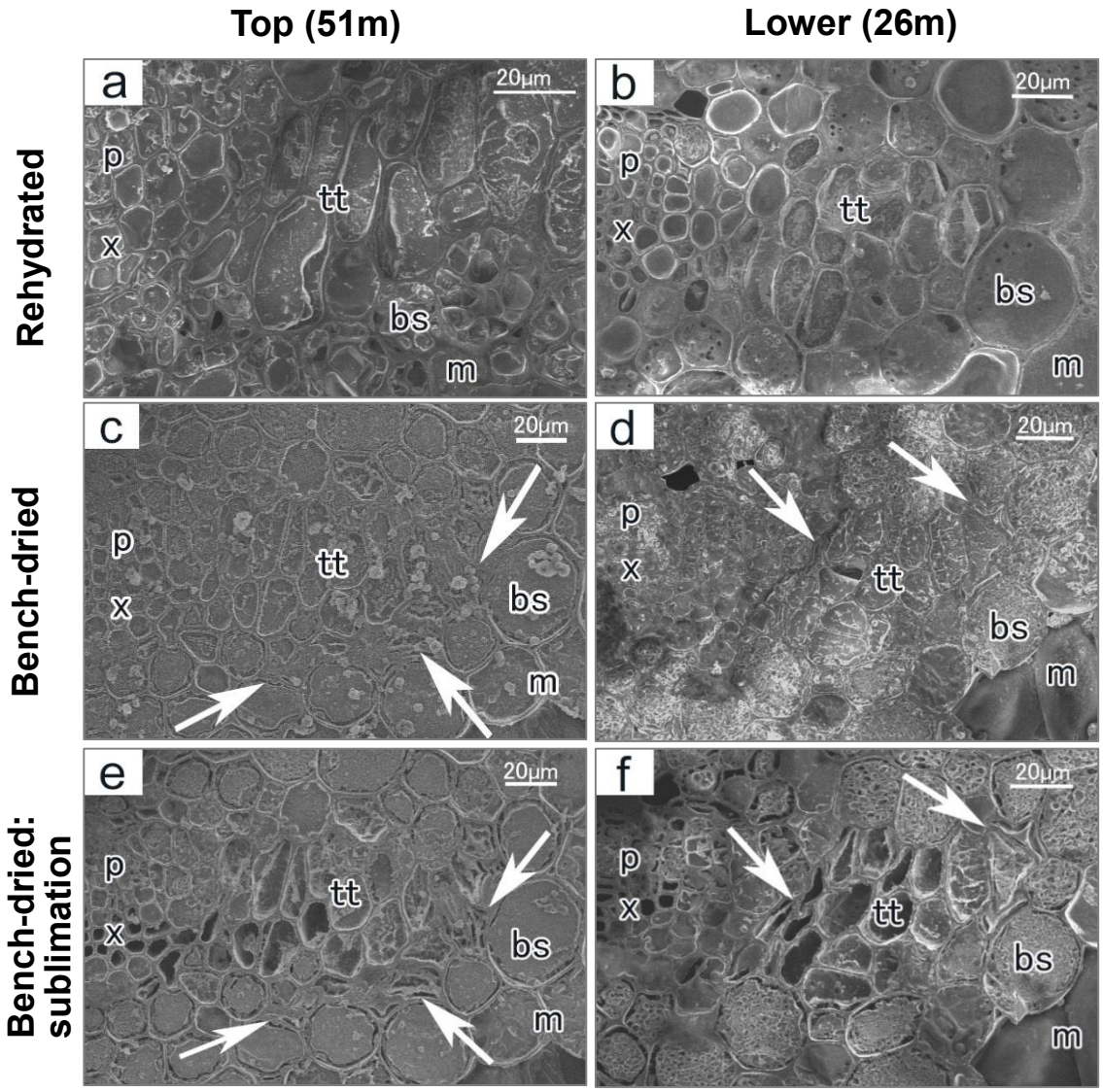

Figure 3.5 Cryo-SEM images of transverse-surface of second-year leaves of *C. japonica*. Treetop (51 m; **a**, **c**, **d**) and lower-crown (26 m; **b**, **d**, **f**) leaves were flash-frozen after rehydration (**a**, **d**) and subsequent bench drying until Ψ_L reached values similar to those at midday in the field (−18.6 and −15.5 MPa for treetop and lower-crown, respectively). (**e**) and (**f**) were taken after deep sublimation of (**c**) and (**d**), respectively. *Arrows* denote examples of deformed transfusion cells. *Abbreviations* m; mesophyll, p; phloem, x; xylem, tt; transfusion tissue, bs; bundle sheath.

3.5 Discussion

In the tallest *C. japonica* trees, Ψ_{tlp} remained constant with height and canopy openness, indicating that drought tolerance of shoots was constant within the crown. On the other hand, C_L and RWC_{tlp} increased with height and canopy openness, which suggested increasing drought avoidance with increasing height and irradiance. Typically, leaves with high C_L have elastic cell walls, which contributes to slow water potential decrease and maintenance of leaf turgor in response to decreasing water content (Salleo 1983). Leaves with elastic cell walls, however, have less ability for water retention than those with hard cell walls (Salleo 1983). To compensate for this, the treetop leaves of *C. japonica* were succulent, having high capacity for water storage relative to evaporative surface area. Such drought avoidance of leaves is important for maintaining productivity at the treetop, where high light and high temperatures cause high vapor pressure deficit. In *Eucalyptus pauciflora*, which were watered after experimentally being exposed to severe water stress, recovery of stomatal conductance occurred much later than stem hydraulic conductance suggesting that in this species, leaf gas exchange is tightly regulated to avoid drought stress (Martorell et al. 2014). Although in *Callitris rhombodieea* (Cupressaceae), transpiration rates recovered rapidly to pre-drought levels after rewatering (Brodribb and Cochard 2009), such regulation may result in reduced photosynthetic rates under constant water stress. While various mechanisms have been suggested as causes for hydraulically induced stomatal limitation in tall trees, in tall *C. japonica*, foliar water storage may be an adaptation, which allows the tallest trees to maintain physiological function in treetop leaves. A similar homeostatic response of Ψ_{tlp} and foliar water storage in treetop leaves was also found in *S. sempervirens* (Chapter 2), and may be a common adaptation to hydraulic constraints in tall Cupressaceae.

In succulent leaves of olive (*Olea europaea* L.) growing in arid regions, osmotic adjustment and development of thick leaves are major adaptations against water stress (Xiloyannis et al. 1999; Bacelar et al. 2004). In the *C. japonica* in this study, osmotic adjustment was not observed but LMA increased with height and light availability. In tall trees, the increase in LMA is driven by height (i.e., water status) more than light availability (Coble et al. 2014) and leaves with greater LMA have less evaporative surface area per dry mass, which prevents decreases in leaf-specific hydraulic conductivity under water stressed conditions (Niinemets 2002; Burgess et al. 2006). In addition, SPAR decreased with height and light availability. In conifer shoots, low SPAR is associated with increasing boundary layer resistance, which decreases evapo-transpirational demand under high vapor pressure deficit (Martin et al. 1999). Low SPAR of treetop leaves also contributes to avoiding the negative effects of excess irradiance on photosynthesis, allows more sunlight to penetrate into the lower crown, and compensates for decreasing photosynthetic rate per leaf dry mass (Niinemets 2002; Ishii et al. 2007; Ishii et al. 2012).

Leaf anatomy also responds to water stress. For example, in the epiphytic plant, *Sarmienta repens*, plants in sun conditions develop thicker, water-storing leaf parenchyma, than those in shade (Godoy and Gianoli 2013). In *C. japonica*, mesophyll anatomy and cuticle thickness did not change with height and light availability (data not shown), while A_{TT} increased. Our cryo-SEM images showed that transfusion cells were flattened when leaf water potential decreased in situ and by experimental dehydration. Deformation of transfusion cells surrounded by bundle sheath may be related to their anatomical characteristics, such as non-uniform shape, tracheary-element-like hollow structure, and cell walls with numerous bordered pits and less lignin deposition compared with normal tracheids (Esau 1997; Bouche et al. 2014). While xylem cell collapse induces

significant reduction in hydraulic conductance (Cochard et al. 2004), in experimentally dehydrated leaves of some conifer species, transfusion cells dehydrate or shrink before embolism occurs in adjacent tracheids in the vascular bundle and contributes to preventing xylem dysfunction (Brodribb and Holbrook 2005; Johnson et al. 2009; Zhang et al. 2014). In this study, it was found that transfusion cells of *C. japonica* were flattened but not fully dehydrated, while no xylem cells were empty or deformed both in situ at mid-day and by experimental dehydration. In addition, recovery of the shape of transfusion cells at predawn as well as after experimental rehydration suggested that deformation of transfusion cells is a reversible process. These observations suggest that, in addition to increasing leaf hydraulic conductance, like leaf veins of broadleaved species (Brodribb et al. 2007), transfusion tissue has functions of both water storage and supply, much like a sponge, absorbing and releasing water according to leaf water status.

The decrease in cross-sectional area of transfusion cells at midday represents the amount of water withdrawn from these cells in response to increasing water demand caused by day-time transpiration. If transfusion tissue volume translates directly to volume of water stored, the slope of the allometric relationship between A_{TT} and S_L would equal 0.5. In this study, the analysis showed that it was 0.28 ($S_L = 521.26\ A_{TT}^{0.28}$, $R^2 = 0.55$, $P = 0.002$), suggesting that in addition to increasing transfusion tissue, mesophyll tissue may contribute to foliar water storage. Because water in mesophyll is easily lost via stomata, dehydration of mesophyll induces decline in photosynthesis as a result of stomatal regulation. Therefore, when transpiration demand increases rapidly, water must be quickly supplied to mesophyll which involves the risk of putting a large load on leaf xylem water potential and inducing xylem embolism. The water stored in transfusion tissue can function as a “circuit breaker” (*sensu* Zhang et al. 2009) against xylem

embolism, protecting the xylem from such excessive loads while maintaining photosynthesis. Thus the plastic response of transfusion tissue may act as a hydraulic buffer preventing disruption of water flow due to such rapid decrease in leaf water potential. More marked deformations of transfusion cells were observed in treetop leaves than in lower-crown leaves suggesting that a greater hydraulic buffer is required for the more water-stressed, treetop leaves.

As with *S. sempervirens* (Oldham et al. 2010; Chapter 2), increasing cross-sectional area of transfusion tissue with height in the tallest *C. japonica* trees reflects increasing capacity for foliar water storage, an anatomical response to increasing water stress. In *S. sempervirens*, cross-sectional area of xylem decreased with height, suggesting decreasing reliance on water transport from roots and that the source of stored water in treetop leaves may not be from roots but from fog or other moisture absorbed via leaf surfaces (Chapter 2). In cloud forests, fog and cloud immersion result in increased photosynthesis, leaf conductance, and xylem water potential in conifers (Simonin et al. 2009; Berry and Smith 2013). In the north coast of California, where *S. sempervirens* occurs, summer fog arising from the Pacific Ocean is an important source of moisture in rainless summer (Dawson 1998; Johnstone and Dawson 2010). In contrast to *S. sempervirens*, cross-sectional area of xylem remained constant with height in *C. japonica*, this may be because the northwest coast of Japan receives more summer rain (ca. 400 mm during Jun, Jul, Aug) than northern California, maintaining soil water supply.

Although stem water storage plays an important role in the water and carbon economy of tall trees (Phillips et al. 2003), experiments using small trees have shown that crown water storage contributes more to whole-tree transpiration rate than the stem (Zweifel et al. 2000). Water storage (hydraulic capacitance) and vulnerability to cavitation of the bole

and branch xylem decrease with height to maintain water transport from root to leaves (hydraulic safety, Domec and Gartner 2001; Burgess et al. 2006; Schulte 2012). Increasing foliar water storage with height could compensate for increasing water demand at the treetop and realize hydraulic homeostasis within the crown. Changes in anatomical structure of a leaf and associated hydraulic properties may be an adaptive mechanism acquired by tall Cupressaceae trees to overcome hydraulic constraints on physiological function with increasing height.

Chapter 4

Water retained in tall *Cryptomeria japonica* leaves as studied by infrared micro-spectroscopy

4.1 Abstract

Recent studies in the tallest tree species suggest that anatomy and tissue structure of tree-top leaves are adapted to the water-limited conditions. In order to examine water retention mechanism of leaves in a tall tree, infrared (IR) micro-spectroscopy was conducted on mature leaf cross-sections of tall *Cryptomeria japonica* from four different heights (19, 31, 43, and 51 m). IR transmission spectra of three leaves at each height were measured and OH and C-O absorption bands were mainly analyzed. The variation in IR spectra of leaf sections from different heights were compared with macroscopic physical measurements such as water contents per unit area or succulence (*S*) and osmotic potentials of saturated leaves ($\Psi_{o, sat}$). Both average OH band area (3700 – 3000 cm^{-1}) of the leaf sections and *S* increased with height. Average C-O band area (1190 – 845 cm^{-1}) increased with height and it was considered that polysaccharides such as pectin and cellulose, the main component of plant cell wall, contributed to this. IR imaging shows localization of the OH and C-O band areas, representing water and polysaccharides respectively, within leaf tissues, which become widespread in mesophyll at the treetop. The OH band can be well fitted by four Gaussian OH components around 3520 (free water), 3380 (pectin), 3300 (cellulose) and 3238 (bound water) cm^{-1}, and all these OH components increase with height without changing their relative proportions. In tall *C. japonica* leaves, OH and C-O contents by IR micro-spectroscopy are found to be increased with height in agreement with physiological water contents. Polysaccharides are supposed to be partly involved in the water retention mechanism in tall tree leaves.

4.2 Introduction

Water transport from root to leaf via xylem in tall trees is realized by the gradient of water potential and supports vital metabolisms like photosynthesis and transpiration (Larcher 2003). As trees become tall, a gradient of light and water availabilities is formed within the crown (Koch et al. 2004; Ishii et al. 2008). At the top of tall trees, light availability for photosynthesis is high, but the water availability is physically constrained by long-distance water transport and increasing gravitational potential and hydrodynamic resistance (Ryan and Yoder 1997; Midgley 2003; Franks 2006).

In Chapter 2, it was found that tree-top leaves of the tallest tree species, *Sequoia sempervirens* (Cupressaceae), have capacity for foliar water storage, which may compensate for constraints on water transport from roots. The same mechanism was also found in the tallest tree species in Japan, *Cryptomeria japonica* (Cupressaceae), due to an increase in transfusion tissue of leaves with height (Chapter 3), which is gymnosperm-specific conducting tissue surrounding the vascular bundle and functions as water storage (Takeda 1931; Hu and Yao 1981; Brodribb et al. 2010; Oldham et al. 2010; Aloni et al. 2013; Chapter 3). These results suggest that anatomical structures of tree-top leaves are adapted to the water-limited conditions. It remains unclear, however, how leaf tissues actually retain water. The elucidation of the water retention mechanism in leaves explains why the water storage at treetop leaves is high, contributing to constant water potential within the crown of tall trees.

Infrared (IR) spectroscopy has been used in plant studies such as plant anatomy, physiology and ecology (Bamba et al. 2002; Dokken et al. 2005; Ribeiro da Luz 2006; Heraud et al. 2007; Martín-Gómez et al. 2015). IR spectroscopy can visualize spatially localized distributions and relative amounts of chemical components corresponding to

plant anatomy at the tissue and cell levels (Dokken et al. 2005; Heraud et al. 2007). Water molecules are considered to be present in various physicochemical states because of varying hydrogen bond distances among them (Maréchal 2007). In IR spectroscopy, OH stretching absorption frequency is known to decrease with decreasing intermolecular hydrogen bond distance (Nakamoto et al. 1955). Therefore, IR OH bands are used for studying hydrogen bonding nature of water molecules associated with bio-macromolecules. Such physicochemical differences of water molecules are considered to affect physiological functions in living systems (Maréchal 2007). However, hydrogen bonding natures of water in tree leaves are not well documented and water retention mechanisms in tall trees in relation to hydrogen bonding structures of water remain mostly unknown.

In this study, IR micro-spectroscopy was conducted on leaf cross-sections of *C. japonica* to investigate water retention mechanisms in the leaves of tall trees based on OH and C-O absorption bands and their distributions in microscopic leaf structures.

4.3 Materials and methods

4.3.1 Sample collection

A 250-year-old *Cryptomeria japonica* tree (height = 51 m, diameter at breast height = 114 cm) at Nibuna-Mizusawa Forest Reserve, Tashirozawa National Forest in Akita Prefecture, Japan (40.08°N, 140.25°E, 200 m altitude from sea level) was selected here as a representative tall mature tree. In November 2013, we accessed the crown of the study tree using single-rope climbing technique. We collected small branches (30−50 cm long) from the outer crown from just below treetop to the lowest living branches at four different heights (51, 43, 31 and 19 m). Sample branches were sealed in black plastic bags and stored in a refrigerator for two weeks.

4.3.2 IR micro-spectroscopy

Second-year fresh leaves (mature leaves) were transversely sectioned at the midpoint between leaf tip and its stem attachment to 24 μm thickness using a sliding microtome equipped with frozen mounting (Fig. 4.1a). Three leaves at each height were sectioned and mounted on an IR transparent CaF_2 crystal (Fig. 4.1b).

In order to study water in these sectioned leaves in equilibrium with the room temperature/humidity conditions, transmission IR spectra of a leaf section at 43 m height were measured at intervals of 60 seconds for 6 hours from 2 hours after sectioning using a Fourier-transform infrared (FT-IR) micro-spectrometer (FTIR-620 + IRT30, Jasco). A 625 μm × 625 μm aperture area in the central part of the leaf cross section (Fig. 4.1 c,d) were monitored with 64 scans at 4 cm^{-1} resolutions in the 4000 – 800 cm^{-1} region at room temperature around 25 ºC. Then at 9, 17 and 23 days after sectioning, transmission IR spectra of all leaf sections at four heights were measured using the same FT-IR micro-

spectrometer with the same aperture in the central part of leaf cross sections with the same measurement conditions as above.

IR micro-spectroscopic imaging was also performed on these leaf sections after 1 day from sectioning using an IR imaging micro-spectrometer (Nicolet iN10MX, Thermo Fisher Scientific) equipped with a 16 channel linear array MCT detector (1 pixel: 25 μm ×25 μm). IR spectra were obtained with 1 scan in the 4000 – 800 cm^{-1} region at 16 cm^{-1} resolutions.

4.3.3 Macroscopic leaf water measurements

We compared the results of IR micro-spectroscopy with macroscopic physical measurements, which are conventionally employed in plant physiology. The leaf water contents can be obtained by subtracting the dry weight, after drying to constant temperature at 65 ^{o}C, from the fresh leaf weights at water saturation. They were normalized by the surface areas of each leaf to obtain water contents per unit area or succulence (S, g H_2O m^{-2}; Bacelar *et al.*, 2004; Ishii *et al.*, 2014). Osmotic potentials of saturated leaves ($\Psi_{o,\,sat}$, MPa) were obtained from the pressure-volume curve using a pressure chamber (Tyree and Hammel 1972; Schulte and Hinckley 1985; Woodruff et al. 2004).

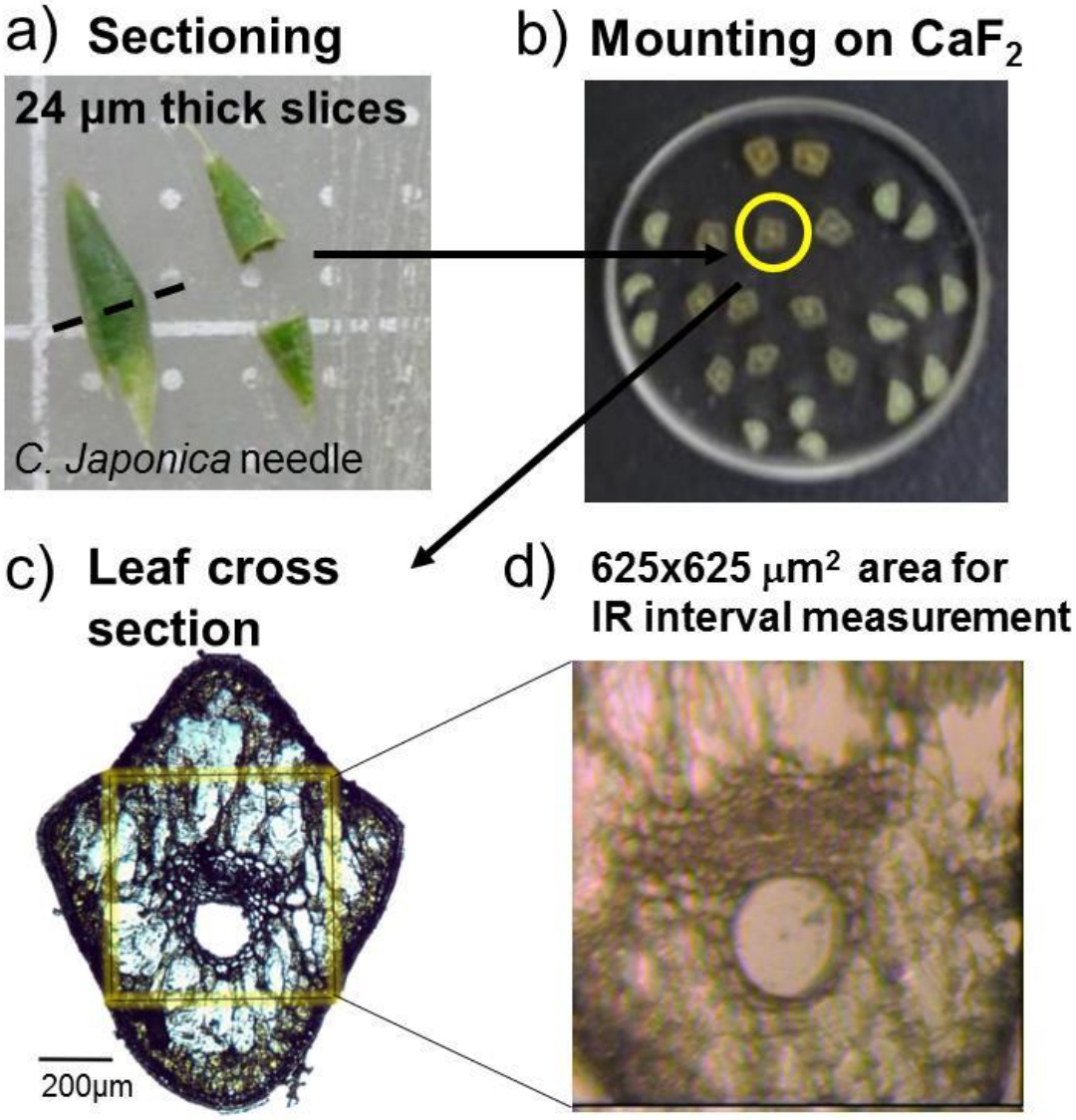

Figure 4.1 (**a**)-(**d**) Procedures for IR micro-spectroscopy of *Cryptomeria japonica* leaves.

4.4 Results and Discussion

4.4.1 IR spectral changes with time after sectioning

Figure 4.2 shows changes in IR transmission spectra during 5 hours at room temperature of the leaf at 43 m height (Fig. 4.1d). A broad band *c.* 3325 cm^{-1} is due to OH stretching vibrations. A band with peaks at 2920 and 2855 cm^{-1} are asymmetric and symmetric stretching of aliphatic CH_2. A band at 1735 cm^{-1} is C=O stretching of carboxyl (COOH). A shoulder *c.* 1645 cm^{-1} can be originated from amide I (C=O stretching) of proteins. A band *c.* 1610 cm^{-1} can be due to COO^- species (deprotonated COOH). A small band at 1545 cm^{-1} might be amide II (C-N-H bending, C-H stretching of peptides). 1415 cm^{-1} can be originated from COO^- of pectin. 1370 cm^{-1} band is due to bending of aliphatic CHs. A small band at 1315 cm^{-1} can be from OH bending in plane of alcohol group. A 1235 cm^{-1} band is corresponding to amide III (C-N-H bending, C-H stretching of peptides). A strong band at 1020 cm^{-1} is due to C-O species in polysaccharides. The assignments of these bands are summarized in Table 4.1.

The changes in IR spectra during 5 hours with a 1 minute interval were mainly attributed to decrease of OH band (Fig. 4.2). In order to examine quantitative changes, band areas of OH (3700 – 3000 cm^{-1}) together with those for CH (3000 – 2785 cm^{-1}) and C-O (1800 – 845 cm^{-1}) were determined and plotted against time (Fig. 4.3a,b). The aliphatic CH and C-O band areas were almost constant during 5 hours of measurement (Fig. 4.3a). On the other hand, the OH band area decreased in the first two hours and then became relatively constant with some fluctuations possibly due to humidity/temperature changes with air conditioning of the experimental room (Fig. 4.3b).

IR spectra of the leaves from four different heights did not show significant changes among 9, 17 and 23 days after sectioning. Since the water decrease of the leaf sections

were limited to the first several hours (Fig. 4.3), their water contents were considered to be in equilibrium with the environmental humidity/temperature. In fact, the OH band areas of the leaves at 9, 17 and 23 days after sectioning showed similar values (Fig. 4.4a).

4.4.2 IR spectra and IR maps of leaf sections from different heights

The averages of the OH and C-O band areas at 9, 17 and 23 days after sectioning were plotted against leaf height along with the maximum and minimum value ranges (Fig. 4.4a,b). The OH and C-O band areas showed an increasing trend with height. The increase in water contents with height appeared to be associated with the increase in sugars.

IR micro-spectroscopic imaging allowed visualization of the spatial distribution of absorption bands for leaf sections from four heights (Fig. 4.5). OH band area (3700 – 3000 cm^{-1}) at 19 m height was large at the central part, corresponding to the vascular bundle and transfusion tissue, and at epidermis (red portions in Fig. 4.5a). The leaves at 31 and 43 m showed similar images. On the other hand, the OH band area for 51 m showed the band increases in the mesophyll regions. C-O band area (1190 – 845 cm^{-1}) at 19 m height was large at vascular bundle and transfusion tissue, and at epidermis (Red portions in Fig. 4.5b). The C-O band area increased with height in mesophyll close to epidermis and finally became widespread at 51 m. As described, localization of water and sugar groups within leaf tissue could be observed using infrared micro-spectroscopy, although the conventional dye staining method (e.g. PAS staining method) to visualize polysaccharides, on the present leaves showed global pink coloration of the entire leaf (data not shown). These increasing microscopic OH and C-O band areas with height are in agreement with the increasing trends observed by the average OH and C-O band area analyses (Fig. 4.4). Figure 4.5c is explained later, in relation to C-O band species.

4.4.3 Comparison with macroscopic physical measurements

We compared the variation in IR spectra of leaf sections from different heights with macroscopic physical measurements, which are conventionally employed in plant physiology. The increasing trend of saturated leaf water contents per leaf surface area (S) with height from around 100 g H_2O m^{-2} at 19 m to around 170 g H_2O m^{-2} at 51 m (Fig. 4.6a) is in agreement with that for the OH band area (Fig. 4.4a). On the other hand, osmotic potentials of saturated leaves ($\Psi_{o,\,sat}$) remained constant with height, around −1.2 MPa (Fig. 4.6b), while the C-O band area increased with height (Fig. 4.4b). Osmotic regulation in leaves is determined by relative amounts of solute concentration between apoplast and intracellular water, and is considered to be controlled mainly by dissolved sugars (Ackerson 1981; Watanabe et al. 2000). In this study, water was considered to increase in both the apoplast and intracellular in leaves with height. Thus, in order to maintain the constant $\Psi_{o,\,sat}$ with height, the concentration of intracellular dissolved sugars could increase with height or the solute concentration in apoplast could decrease. Another factor that could affect the increase of C-O band area with height, is that the treetop leaves produce more photosynthetate, such as starch, than the lower leaves. Further studies including chemical analysis of leaves from different heights are needed to answer these questions. The plant cell wall consists of various polysaccharides such as cellulose, hemicellulose and pectin and their proportions change for different species (Evert, 2006; Fukushima *et al*., 2011). As these polysaccharides are non-soluble in water, but are hydrophilic, if the increase in the C-O band area with height reflected the increase in polysaccharides, these may contribute in part to water retention in tree-top leaves.

4.4.4 OH band components in the OH stretching region

In order to discriminate different water and sugar species at different heights, difference IR spectra were investigated. The IR spectrum of leaf section at 19 m height was subtracted from those at 31, 43 and 51 m heights to examine differences in water and sugar species (Fig. 4.7a). The subtraction was conducted by applying a coefficient to the 19 m spectrum so as to obtain the absorbance zero at 3000 cm^{-1}, which is considered as a stable absorption minimum (Fig. 4.7b; 51m spectrum: 51 m – 19 m x 1.98, 43 m: 43 m – 19 m x 1.2, 31 m: 31 m – 19 m x 1.33). In the OH stretching region, a positive band *c.* 3520 cm^{-1} is observed for 31 m leaf and it increases for higher leaves (Fig. 4.7b). Another band *c.* 3250 cm^{-1} also appears to increase for higher leaves (Fig. 4.7b).

In order to examine OH bands of representative polysaccharides, IR transmission spectra of cellulose and pectin films were measured (Fig. 4.7c). OH and C-O bands show differences for cellulose and pectin. The 3300 cm^{-1} band is considered to be due to OH groups in cellulose, while the 3380 cm^{-1} band is due to –COOH groups in pectin.

The OH band positions observed in the difference spectra of leaves (3520, 3250 cm^{-1}) and in the cellulose and pectin films (3300, 3380 cm^{-1}) were used as initial positions for fitting the OH bands of leaves by four Gaussian bands without fixing the band positions (Fig.4.8a). The fitting results for three samples at each height showed relatively good fits with four Gaussian components with average band positions at 3529, 3412, 3307 and 3209 cm^{-1}. The representative fitting result is shown in Figure 4.8a. Average band areas of three samples at each height were plotted against the height with the maximum and minimum value ranges for each Gaussian component (Fig. 4.8b). The average band area increased with height. On the other hand, the percentages of average band areas of three samples are mostly unchanged for different heights (Fig. 4.8c). The band area of 3380

cm^{-1} (–COOH groups in pectin-like species) and 3250 cm^{-1} (water molecules with shorter H bonds) components occupy about 30%, respectively, and that of 3520 cm^{-1} (water molecules with longer H bonds) and 3300 cm^{-1} (OH groups in cellulose-like species) occupy about 20%, respectively (Fig. 4.8c). The water molecules with shorter H bonds ('bound water') are more abundant than those with longer H bonds ('free water') (Fig. 4.8c).

With increasing height, the amount of water in leaves of tall *C. japonica* increase, while the water species retained in leaves seems to be similar among different heights. These water species are considered to be retained by polysaccharides such as pectin and cellulose.

4.4.5 Biomolecules contributing to water retention

The IR spectra of the cedar leaves showed the presence of bands *c.* 1735 cm^{-1} (COOH), 1610 and 1415 cm^{-1} (COO^-), 1315 cm^{-1} (alcohol OH) and 1020 cm^{-1} (C-O-C) besides amides (I: 1645 cm^{-1}, II:1545 cm^{-1} and III:1235 cm^{-1}), CHs (2920, 2855, 1370 cm^{-1}) and OH bands (3325 cm^{-1}) (Figs. 4.2 and 4.7a; Table 4.1). These bands, in particular 1735, 1610, 1415 and 1020 cm^{-1} bands, are similar to those for pectin (Fig. 4.7c). On the other hand, 1735, 1610 and 1415 cm^{-1} bands are not clear for cellulose. Therefore, the main polysaccharide component in the leaves is considered to be pectin-like materials.

In the 1800 – 1000 cm^{-1} region of the difference spectra from the leaf at 19 m height, several positive bands are observed (Fig. 4.7b). The positive bands generally increasing with height include contributions mainly from 1) amide I (1670 cm^{-1}) and II (1550 cm^{-1}) bands of proteins present in mesophyll (possibly photosynthetic protein such as Rubisco), 2) COO^- of pectin (1415 cm^{-1}) and 3) C-O-C (1170 and 1120 cm^{-1}) of polysaccharides

(Fig. 4.7b).

1) The observed increase of proteins with height is likely to reflect high-light acclimation for increasing photosynthetic proteins such as Rubisco (Warren & Adams, 2001). 2) The increase of COO^- possibly linked to pectin at the treetop leaves can be explained by decarboxylation of –COOH and its binding to Ca^{2+} in the cell forming Ca^{2+} – ^-OOC linkage for cell walls of leaf tissue (Fig 4.9a; Demarty et al. 1984; Liners et al. 1989; Dunand et al. 2002). The presence of positive bands from 1730 to 1610 cm^{-1} (Fig. 4.7c) can also be explained by this conversion of COOH (1740 cm^{-1}) to COO^- (1610 cm^{-1}). 3) Concerning the C-O-C bands, the ratio of two bands of polysaccharides (the peak height ratios 1120:1170 cm^{-1}) increased with height in the IR maps (Fig. 4.5c). In the treetop leaves (51m), the areas with large 1120:1170 cm^{-1} ratios surround the vascular bundle and transfusion tissue, which have water transport and storage functions, respectively (Evert, 2006; Brodribb *et al.*, 2007; Azuma et al. 2015). On the other hand, amounts of water and polysaccharides increased in surrounding outer regions of mesophylls (Fig. 4.5a,b). The increase of the peak height ratios 1120:1170 cm^{-1} might be related to some changes in polysaccharides for the effective radial transportation and retention of water in higher leaves. The band around 1145 cm^{-1} for pectin (Fig. 4.7c) can be shifted to the lower wavenumber region by hydrogen bonding of adsorbed water molecules to C-O species. Therefore, the increase in the peak height ratios 1120:1170 cm^{-1} with height for mesophyll regions in the IR map (Fig. 4.5c) can be tentatively explained by a shift of C-O bonds by hydrogen bonding to water molecules.

The study shows that, in tall *C. japonica* leaves, both OH and C-O band areas increase with height in agreement with physiological measurements of leaf water content. IR imaging shows localization of water and polysaccharides around the vascular bundle,

transfusion tissue and in mesophyll adjacent to the epidermis of leaf transverse sections, and they became widespread in mesophyll at the tree-top. Based on these results, it was inferred that polysaccharides may contribute in part to water retention. The present results suggest the following working hypothesis for water retention mechanism by polysaccharides (Fig. 4.9):

1) Polysaccharide content (e.g., pectin) is higher for leaves in the upper crown.
2) Their carboxyl groups (COOH) become deprotonated (COO^-) and bound to Ca^{2+} in the cell to form Ca bridges linking pectin molecules. (Fig. 4.9a)
3) Water molecules are then bound in the Ca-linked pectin molecules by hydrogen bonding to C-O-C and C-OH. (Fig. 4.9b)

Detailed studies on water absorption by constituent biomolecules (polysaccharides such as pectin, cellulose, hemi-cellulose, lignin, proteins such as Rubisco and lipids) are needed for further understanding of the mechanism of foliar water storage in tall trees. For example, in order to examine above working hypothesis, water adsorption experiments to pectin with and without Ca bridges at different relative humidity conditions should be conducted. Then by comparing these results with the same type of adsorption experiments for the tree leaves, adsorbed water species and functional groups interacting with water can be elucidated. The importance of polysaccharides such as pectin for the water retention in tall tree leaves will be then confirmed.

Table 4.1 Assignments of infrared bands observed in transmission spectra of the leaf section at 43 m (Fig. 4.2), in the difference spectra from the 19 m spectrum for the leaves at 51, 43 and 31 m (Fig. 4.7b), in the spectra for pectin and cellulose films (Fig. 4.7c) and in the OH bands of the leaves (Fig. 4.8). Abbreviations designate the followings. ν_{as}: asymmetric stretch, ν_s: symmetric stretch, δ_{as}: asymmetric deformation (bend), δ_s: symmetric deformation (bend).

Figure No.	Wavenumber (cm^{-1})	Assignment
7b, 8	3520	v(O-H) (long H bond) (Kubo & Kalda. 2005; Fackler et al., 2010)
7c, 8	3380	v(O-H) (COOH of pectin) (Synytsya et al. 2003)
7c, 8	3300	v(O-H) (OH of cellulose) (Chung et al. 2004, Yang et al. 2007)
7b, 8	3250	v(O-H) (short H bond) (Fackler et al., 2010)
2	2920	ν_{as}(C-H) from aliphatic CH_2 (Painter et al., 1981; Tonoue et al., 2014)
2	2855	ν_s(C-H) from aliphatic CH_2 (Painter et al., 1981; Tonoue et al., 2014)
7c	1740	v(C=O) (COOH of pectin) (Kacurakova & Wilson, 2001; Heraud et al., 2007; Synytsya et al. 2003; Szymanska-Chargot & Zdunek 2013)
2	1735	v(C=O) from carbonyl groups of lignin and lipids (Painter et al., 1981;Labbe et al., 2005; Heraud et al., 2007; Tonoue et al., 2014)
7b	1730	
7b	1670	v(C=O) from peptides (H-N-C=O) (amide I of proteins) (Heraud et al., 2007; Fabian & Naumann, 2012)
2	1645	
2, 7b	1610	v(C=O) of lignin, ν_{as}(COO-) of pectin (Kacurakova & Wilson, 2001; Labbe et al., 2005; Heraud et al., 2007; Synytsya et al. 2003)
7b	1550	v(C-H) and δ(N-H) from amide II of proteins (Heraud et al., 2007; Fabian & Naumann, 2012)
2	1545	
7b	1515	v(C=C) of lignin (Heraud et al., 2007)

7b, 7c	1450-1440	$\delta_{as}(CH_3)$ and $\delta_{as}(CH_2)$ of proteins, lipids and lignin (Painter et al., 1981; Heraud et al., 2007)
2, 7b, 7c	1415	$\nu_s(COO^-)$ of pectin (Kacurakova & Wilson, 2001; Heraud et al., 2007; Synytsya et al. 2003; Szymanska-Chargot & Zdunek 2013)
7b	1375	δ(C-H) from CH_3 groups (Painter et al., 1981; Tonoue et al., 2014)
2, 7c	1370	$\delta_s(CH_3)$ and $\delta_s(CH_2)$ of proteins, lipids and lignin (Heraud et al., 2007)
7b	1320	ν(C-H) and δ(N-H) from amide III of proteins (Heraud et al., 2007; Fabian & Naumann, 2012)
2	1235	
2	1315	δ(O-H) in plane from alcohol groups of carbohydrates (Marechal & Chanzy, 2000; Fackler et al., 2010)
7b	1270	ν(C-C) and ν(C-O) of carbohydrates and lignins (Heraud et al., 2007)
7b	1170	ν_{as}(C-O-C) from glycoside of polysaccharides (Liang & Marchessault, 1959; Marechal & Chanzy, 2000; Fackler et al., 2010)
7c	1145	ν_{as}(C-O-C) of pectin (Heraud et al., 2007; Synytsya et al. 2003)
7b	1120	ν_{as}(C-O-C) in ring of polysaccharides (Liang & Marchessault, 1959; Kacurakova et al., 1999; Marechal & Chanzy, 2000)
2, 7c	1020	ν(C-O) of polysaccharides (Marechal & Chanzy, 2000; Fackler et al., 2010)

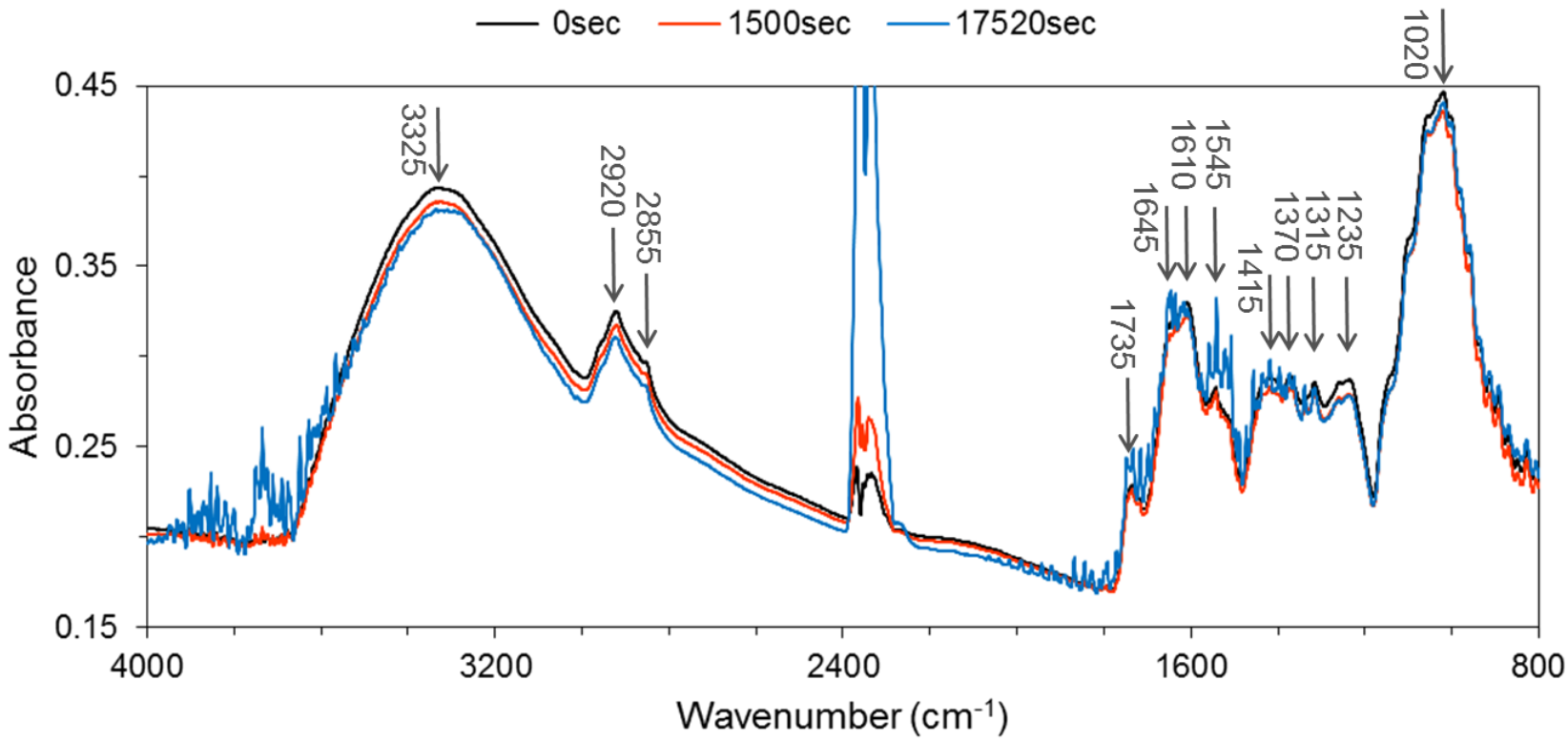

Figure 4.2 Changes with time (0, 1500 and 17520 seconds) in IR transmission spectra of a leaf at 43 m height from 2 hours after sectioning.

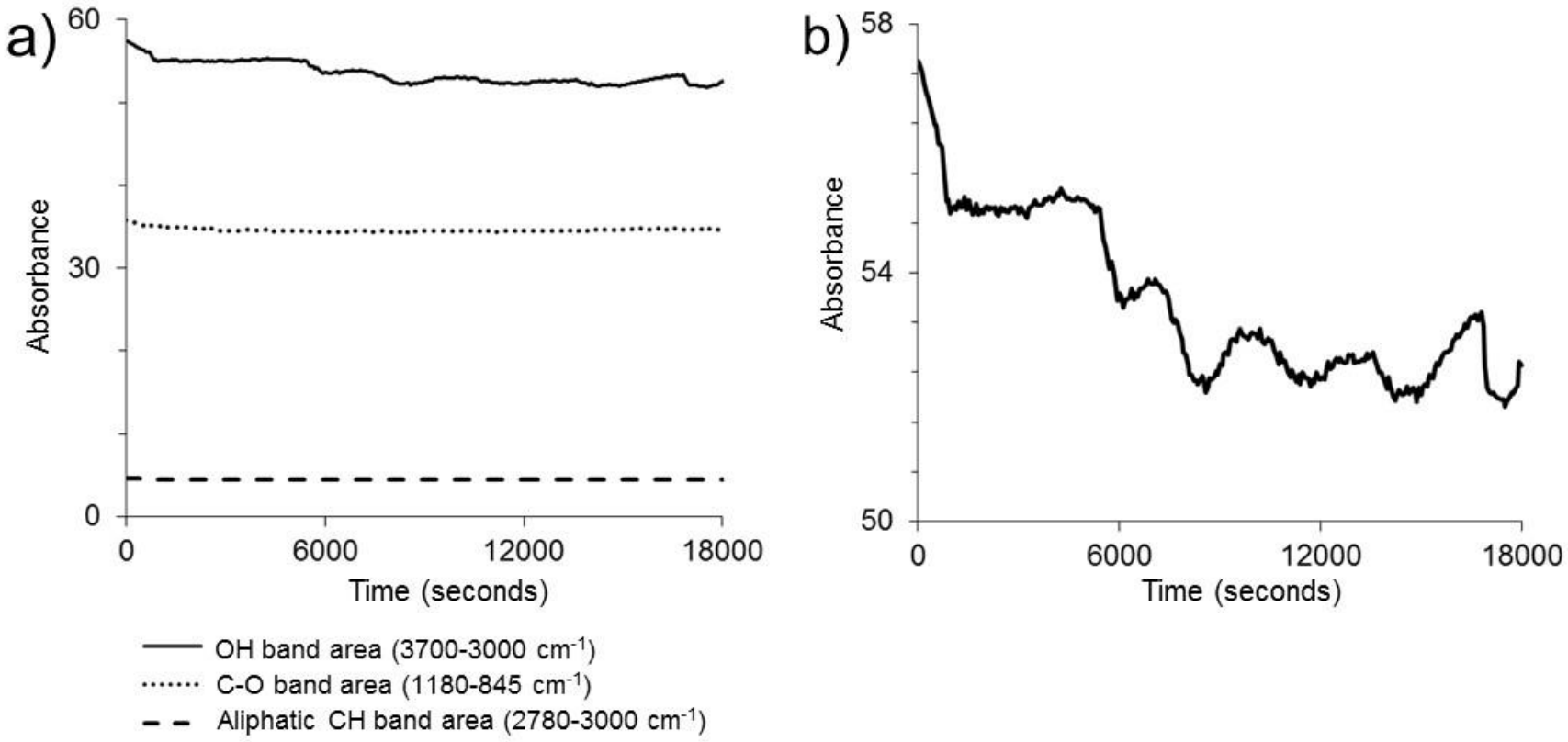

Figure 4.3 (**a**) Changes with time in OH, C-O and CH band areas during 5 hours in IR transmission spectra of the leaf at 43 m (Fig. 2). (**b**) Close-up of the OH band area decrease with time.

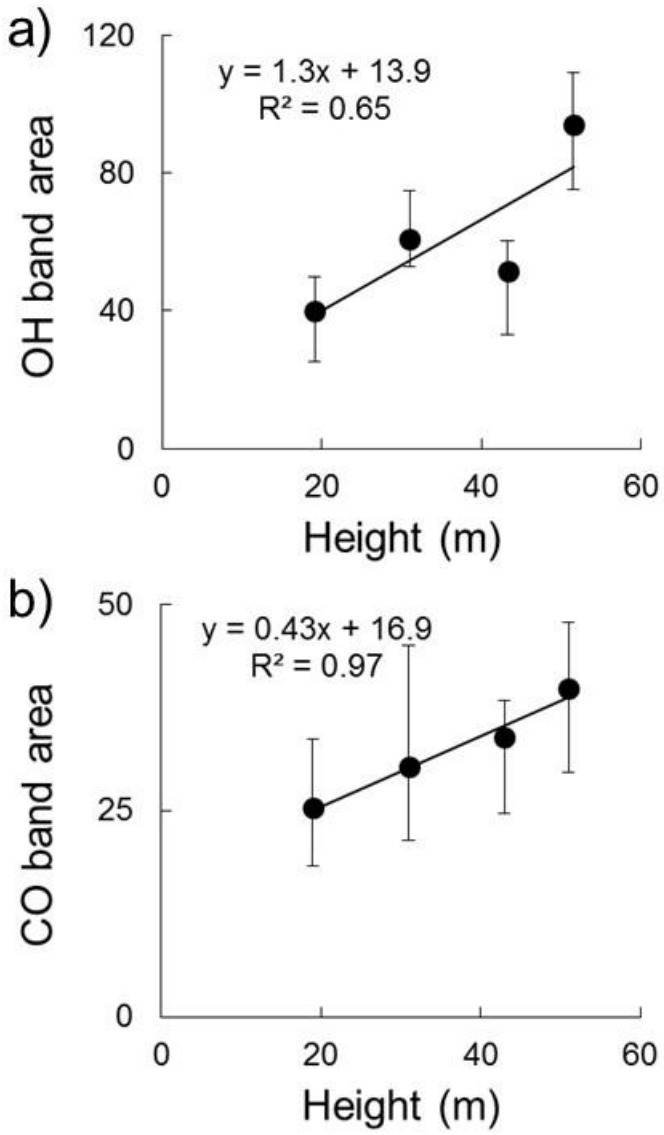

Figure 4.4 Changes with height in averages IR band areas of (**a**) OH and (**b**) C-O of the leaf sections at 9, 17 and 23 days after sectioning. Error bars indicate maximum and minimum value ranges.

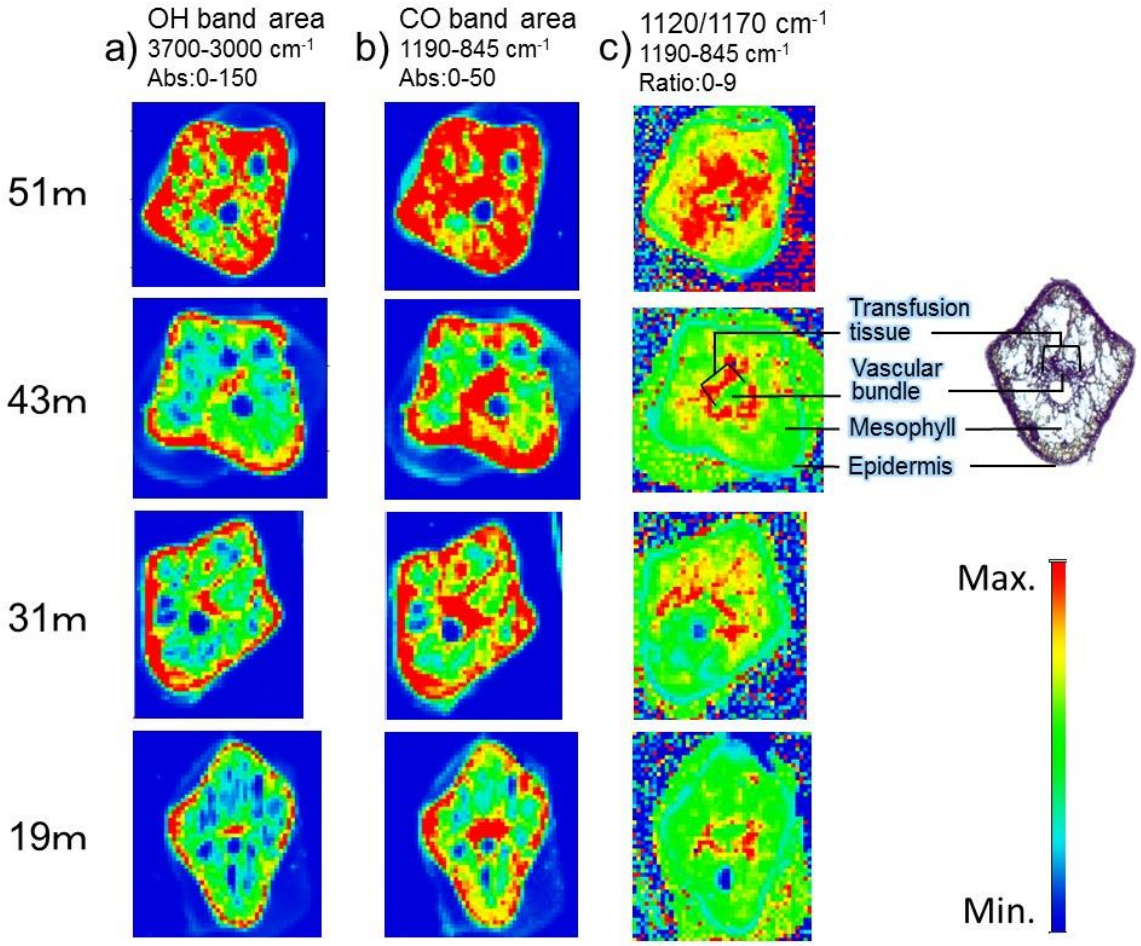

Figure 4.5 IR micro-spectroscopic mapping images of leaf sections from different heights (19, 31, 43 and 51 m) for (**a**) OH (3700-3000 cm^{-1}) band area, (**b**) C-O (1190-845 cm^{-1}) band area, and (**c**) peak height ratios 1120:1170 cm^{-1} (baseline: 1190-845 cm^{-1}).

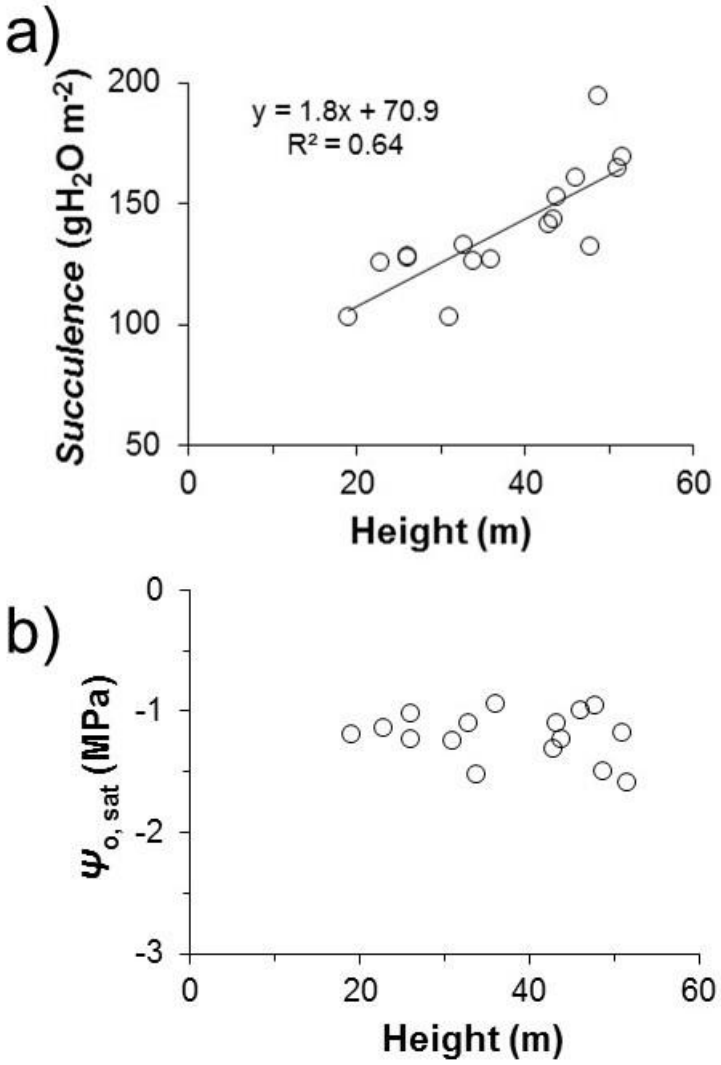

Figure 4.6 Changes with height in macroscopic physical data. (**a**) Water content per unit leaf surface area at water saturation (Succulence, *S*). (**b**) Osmotic potentials of water-saturated leaves ($\Psi_{o, sat}$).

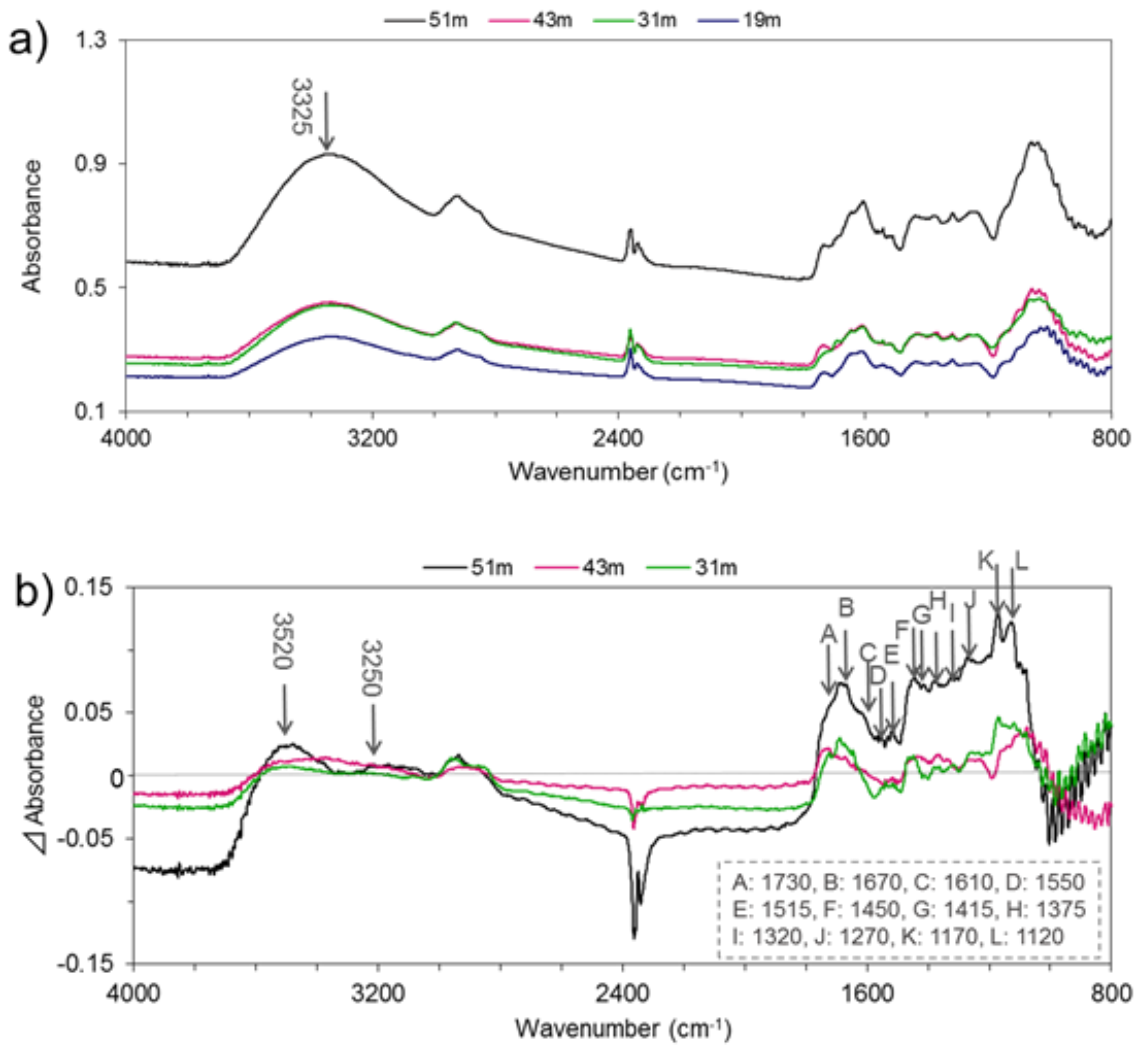

Figure 4.7-1 (**a**) IR transmission spectra of the leaves at 19, 31, 43 and 51 m, 23 days after sectioning. (**b**) Difference spectra from the 19 m spectrum with a coefficient so as to obtain the absorbance zero at 3000 cm^{-1} (51m spectrum: 51 m – 19 m x 1.98, 43 m: 43 m – 19 m x 1.2, 31 m: 31 m – 19 m x1.33).

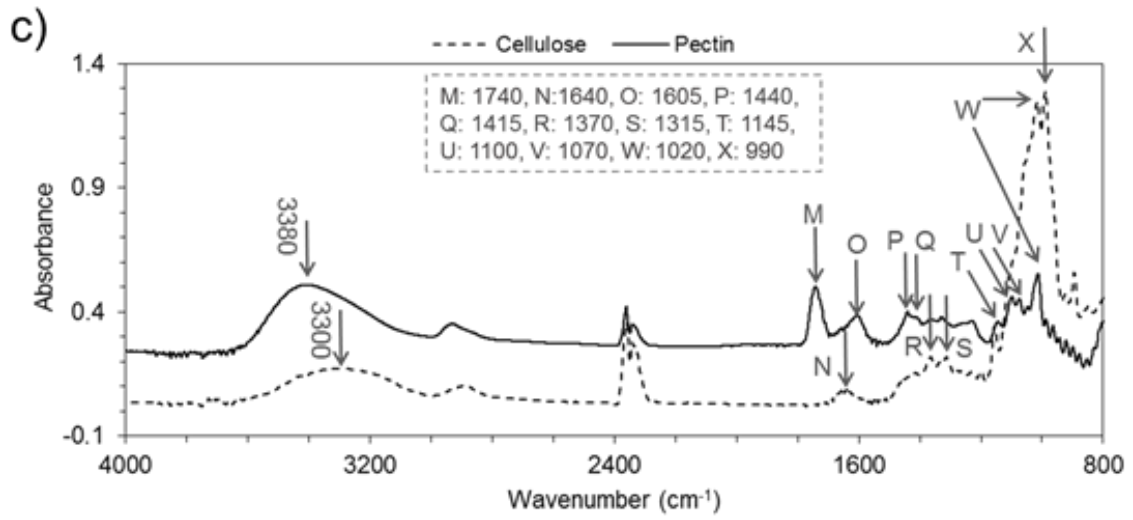

Figure 4.7-2 (**c**) IR transmission spectra of a cellulose film and a pectin film. The absorbance of cellulose was multiplied by 20 for comparison with that of pectin.

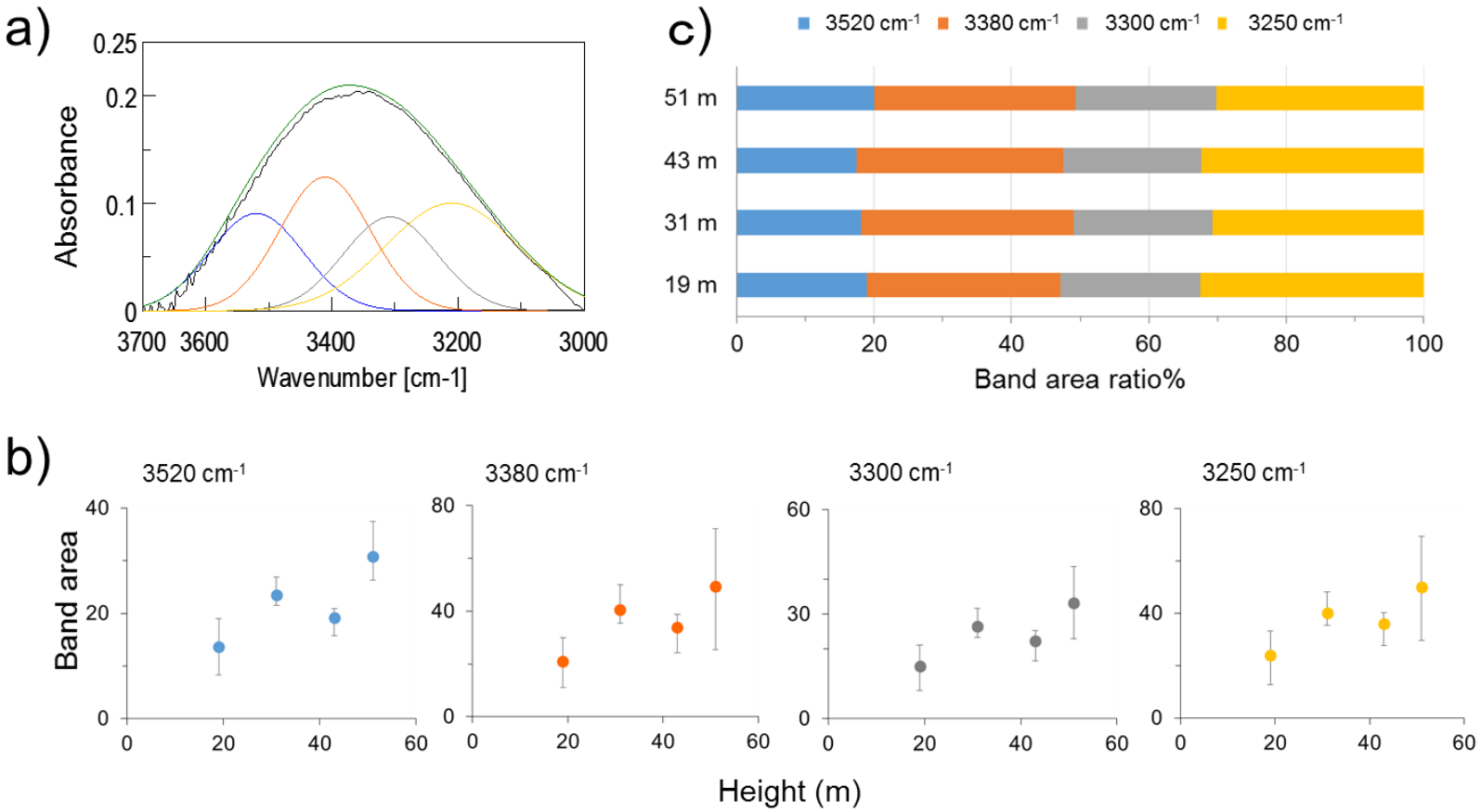

Figure 4.8 (**a**) A representative curve fitting result of OH band by four Gaussian components with initial band positions at 3520, 3380, 3300 and 3250 cm^{-1}. (**b**) Changes with height in band areas of four Gaussian components. Error bars indicate maximum and minimum value ranges. (**c**) The percentage compositions of four band areas in leaves from different heights.

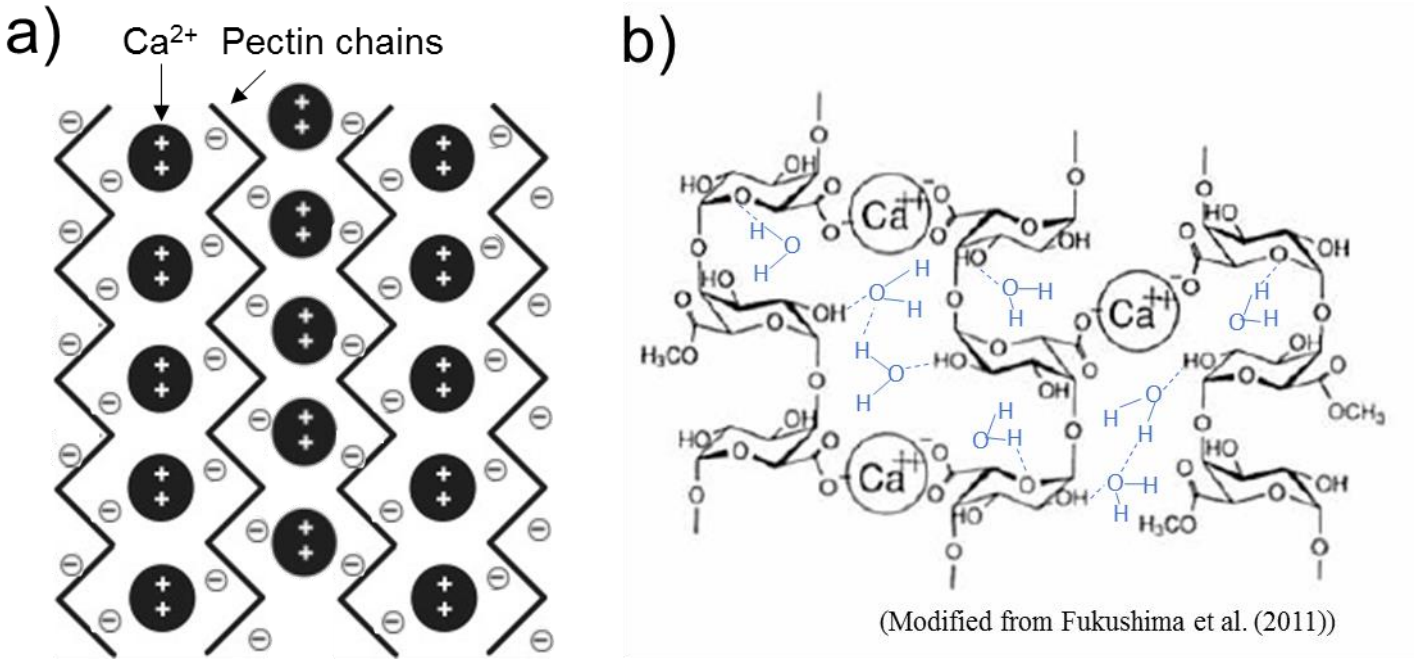

Figure 4.8 The working hypothesis for water retention mechanism in leaves of tall tree. (**a**) The carboxyl groups (COOH) become deprotonated (COO-) and bound to Ca^{2+} in the cell to form Ca bridges linking pectin chains. (**b**) Water molecules are then bound in the Ca-linked pectin molecules by hydrogen bonding to C-O-C and C-OH.

Chapter 5

General discussion

5.1 Study summary

In these studies, the single rope technique (Laman 1995; Ishii 2000) made it possible to directly measure the physiological functions of leaves and environmental conditions at treetop in tall trees without huge facilities such as canopy tower. In order to elucidate the physiological factor limiting the height growth in tall trees, multidisciplinary approaches are needed, in addition to conventional tree physiological techniques. In this study, I incorporated investigation of tissue structures related to physiological functions by anatomical measurements and physicochemical properties of water in leaf tissue by spectrometry measurements.

Three main results of this study are as follows:

1) The effects of water stress on leaves within the crown is constant and independent of height

As indicated by results of the physiological measurements on leaves sampled at various heights from treetop to the lowest branches in *Sequoia sempervirens* and *Cryptomeria japonica*, constant water potential at turgor loss point reflected that the effects of water stress on leaves was constant. In contrast, leaf capacitance increased with height. As the leaves became smaller with height, light-intercepting area for photosynthesis decreased, while saturated water content per unit transpirational area increased. Thus it was suggested that hydraulic constraints at treetop was compensated by increased capacitance of leaves. In *S. sempervirens*, these results were observed in both of the different climatic regions, dry and humid. The leaves were capable of storing water equivalent to five-times and four- times of the amount of daily transpiration in *S. sempervirens* and *C. japonica*, respectively.

2) Tissue structure of leaves (transfusion tissue) contributes to increasing the leaf capacitance at treetop

As indicated by results of anatomical measurements in transverse sections of leaves in *S. sempervirens* and *C. japonica*, the cross-area of transfusion tissue, which is specific to gymnosperms, increased with height. As indicated by observation of both leaf tissues and water using cryo-SEM after deep freezing by liquid nitrogen, the shape of transfusion cells deformed containing water at midday and recovered the original shape by the rehydration until predawn. This suggests that such reversible changes enable transfusion tissue to function as both the sink for storing water and the source for supplying water to leaves. In *S. sempervirens* and *C. japonica*, it was suggested that functional structures of leaves change with height, giving priority to water storage in order to maintain water conditions of leaves for the constant of physiological functioning at treetop and the optimum trade-off in resource allocation between photosynthetic apparatus versus water storing tissue determine maximum tree height.

3) The visualization of the distribution of water and sugar-species in the leaf transverse sections

Infrared (IR) micro-spectroscopy was conducted on mature leaf cross-sections of tall *C. japonica* to examine water retention mechanism of leaves. The variation in OH band area with height corresponds to macroscopic physical measurements such as water contents per unit area. IR imaging showed that the quantity and localization in leaf cross-section of water and sugar-species like polysaccharides, which become widespread in mesophyll at treetop. The present results suggested the following working hypothesis for water retention mechanism that water molecules are then bound

in the Ca-linked pectin molecules. Polysaccharides can contribute to water retention in tall tree leaves.

Based on the above results, I propose the “hydraulic homeostasis hypothesis” for the mechanism of height-growth limitation in tall trees, which includes a new concept of physiological adaptation (as opposed to the conventional, physiological constraint) to water stress in tall *S. sempervirens* and *C. japonica* (Fig 5.1).

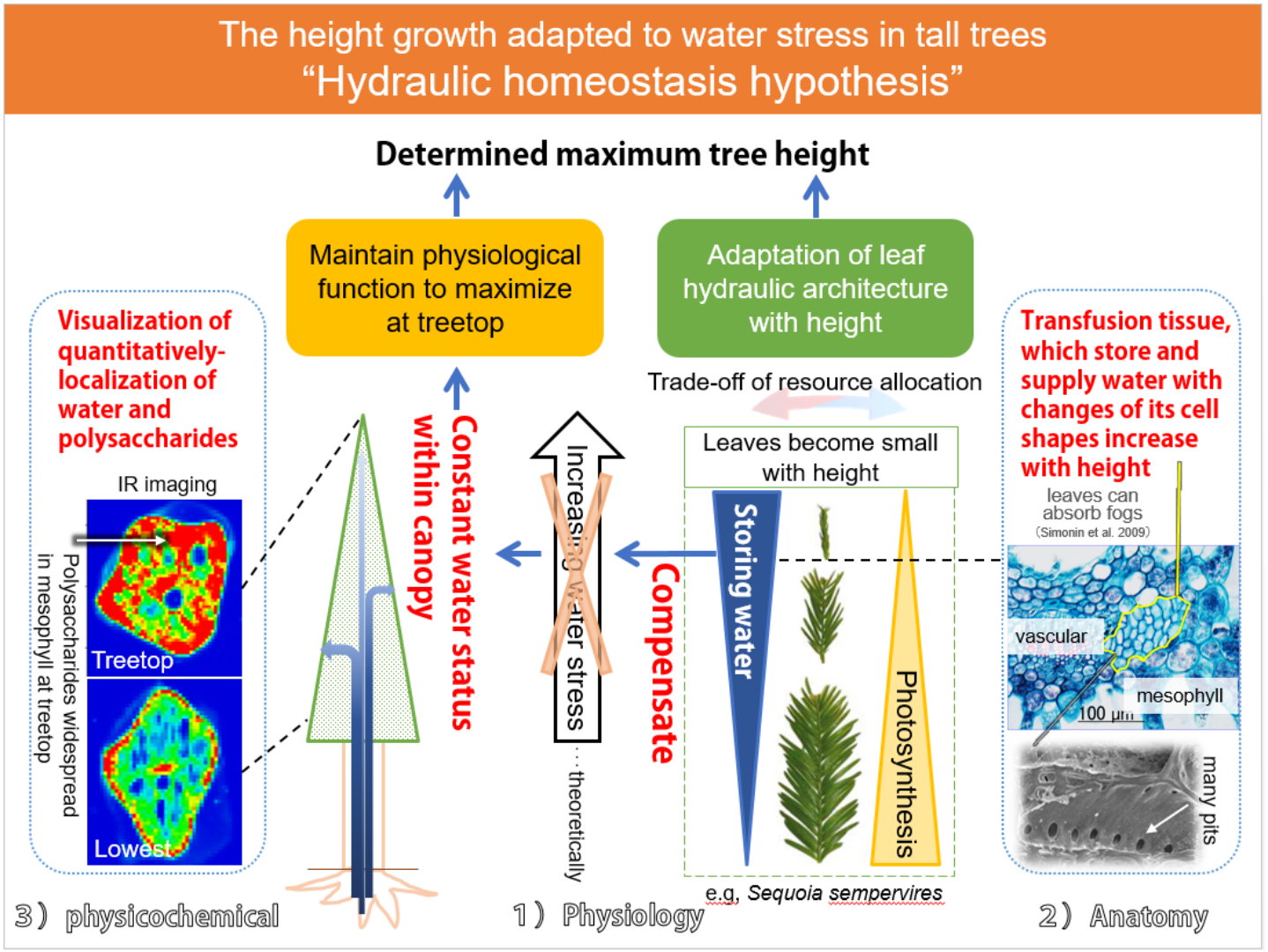

Figure 5.1 Conceptual diagram illustrating homeostasis of crown structure and function

5.2 Homeostasis of crown structure and function in tall trees: A hypothesis

Theoretical criticisms of the hydraulic limitation hypothesis (e.g., Becker et al. 2000) were followed by empirical evidence suggesting that height growth limitation is not as simple as the hypothesis proposes. For example, stomatal limitation alone does not explain reductions in height growth (Niinemets 2002) and various compensating mechanisms have been found that maintain hydraulic conductance with increasing height (McDowell et al. 2002; Barnard and Ryan 2003). These include lower leaf water potential at canopy top during times of water stress (Barnard and Ryan 2003), greater sapwood area per unit leaf area (McDowell et al. 2002), greater hydraulic capacitance (water storage) (Phillips et al. 2003; Meinzer et al. 2006; Scholz et al. 2011), and hydraulic acclimation is including alteration of hydraulic architecture such as allocation between foliage and fine roots (Magnani et al. 2000), xylem tapering (Zaehle 2005), production of new vessels in xylem at dry seasons (Uemura et al. 2004).

While increases in leaf area may compound hydraulic limitation in large trees in the long term (Phillips et al. 2003), there is evidence that short-term adjustments in leaf area could maintain homeostasis of leaf specific conductivity and carbon assimilation (Sobrado 2003). Theoretically, stomatal regulating as 'isohydric' behavior produces near-homeostasis in leaf water potential when the plant's hydraulic system is operating close to capacity (Buckley 2005). Both long-term structural acclimation and short-term physiological regulation relate to change the levels of hydraulic conductance significantly (Mencuccini 2003). In desert shrubs, for example, homeostasis of leaf water potentials between the leeward and windward sides is maintained by changes in both leaf physiological and morpho-anatomical traits (Iogna et al. 2013). The existence of similar transport sufficiency (leaf-area normalized whole-plant hydraulic conductance) among

various tree species including both angiosperms and conifers (Andrade et al. 1998; Becker et al. 1999), suggests evolution of adaptation to maintain hydraulic homeostasis. Becker raised the importance of evolutionary selection for increasing fitness of a species and that natural selection should select for species able to adjust resource allocation where height growth enhances tree survival and reproductive success (Becker et al. 2000). In the neotropical savanna trees, the patterns of water uptake and access to soil water during the dry seasons seemed to mainly determine wood density, which constrained evolutionary options related to plant water economy and hydraulic architecture, leading to functional convergence (Bucci et al. 2004).

The existence of mechanisms that compensate hydraulic limitation reflects the importance of maintaining leaf water status for physiological functioning. This is true for all parts of the crown of a large tree. Theoretical and empirical studies on hydraulic architecture suggests homeostasis of leaf water status within the crown of a tree (Tyree et al. 1983) and hydraulic models predict hydraulic conductance and transpirational demand should be in balance, and thus constraints on water transport should be compensated to maintain leaf water status (Whitehead et al. 1984). Such hydraulic homeostasis models have proposed that constant water supply to all leaves within a tree could be realized by tapering of xylem conduits, which maintains total resistance to water transport constant throughout all the tree (West et al. 1999). Xylem anatomy such as pit membranes related to trade-off between conducting efficiency and cavitation by drought (Hacke and Sperry 2001; Schulte 2012). Recently, it has been discovered that that aquaporins, which is water channel proteins for facilitating water transport across cell membranes, mediate changes in root and leaf hydraulic conductance (Hacke 2014). In hybrid popular plants subjected to reducing the relative humidity or increasing the light intensity, root water flow

increased with increasing the transcript abundance of aquaporin genes in roots (Laur and Hacke 2013). In drought-stressed *Picea plauca*, when exposed to high humidity, water absorption started and up-regulation of aquaporins, observed in the endodermis-like bundle sheath, phloem cells and transfusion parenchyma of needles, coincided with embolism repair in stem xylem aquaporins (Laur and Hacke 2014). Besides studies on the structure differentiation of leaves, a better knowledge of the function and regulation of the numerous aquaporine homologs expressed in leaves is also critically needed (Prado and Maurel 2013).

Because treetop leaves receive the greatest amount of sunlight within a crown, they may be hydraulically prioritized to realize high productivity (Sellin and Kupper 2005, 2007; Otoda and Ishii 2009). It is likely, however, that hydraulic compensation is coupled with some cost in terms of resource allocation (i.e. carbon costs) (Barnard and Ryan 2003). In this study, foliar water storage increased with height in *S. sempervirens* and *C. japonica*, suggesting trade-off in resource allocation between photosynthetic apparatus versus water-storing tissue. Maximum height may therefore be determined by the outcome of this trade-off (Fig. 5.1). Future research should focus on adaptive mechanisms that compensate for hydraulic constraints and how the tallest trees push the limits to tree height.

Reference

Ackerson RC. 1981. Osmoregulation in Cotton in Response to Water Stress: II. Leaf Carbohydrate Status in Relation to Osmotic Adjustment. Plant Physiology 67: 489–493.

Aloni R, Foster A, Mattsson J. 2013. Transfusion tracheids in the conifer leaves of *Thuja plicata* (Cupressaceae) are derived from parenchyma and their differentiation is induced by auxin. American Journal of Botany 100: 1949–1956.

Ambrose AR, Sillett SC, Dawson TE. 2009. Effects of tree height on branch hydraulics, leaf structure and gas exchange in California redwoods. Plant, Cell and Environment 32: 743–757.

Ambrose AR, Sillett SC, Koch GW, Van Pelt R, Antoine ME, Dawson TE. 2010. Effects of height on treetop transpiration and stomatal conductance in coast redwood (*Sequoia sempervirens*). Tree Physiology 30: 1260–1272.

Andrade LJ, Minzer FC, Goldstein G, Holbrook NM, Cavelier J, Jackson P, Silvera K. 1998. Regulation of water flux through trunks, branches, and leaves in trees of a lowland tropical forest. Oecologia 115: 463–471.

Bacelar EA, Correia CM, Moutinho-Pereira JM, Goncalves BC, Lopes JI, Torres-Pereira JMG. 2004. Sclerophylly and leaf anatomical traits of five field-grown olive cultivars growing under drought conditions. Tree Physiology 24: 233–239.

Bamba T, Fukusaki EI, Nakazawa Y, Kobayashi A. 2002. In-situ chemical analyses of trans-polyisoprene by histochemical staining and Fourier transform infrared microspectroscopy in a rubber-producing plant, *Eucommia ulmoides* Oliver. Planta 215: 934–939.

Barcikowski W, Nobel PS. 1984. Water relations of cacti during desiccation: distribution of water in tissues. Botanical Gazette 145: 110–115.

Barclay HJ, Goodman D. 2000. Conversion of total to projected leaf area index in conifers. Canadian Journal of Botany 78: 447–454.

Barnard HR, Ryan MG. 2003. A test of the hydraulic limitation hypothesis in fast-growing *Eucalyptus saligna*. Plant, Cell and Environment 26: 1235–1245.

Bartlett MK, Scoffoni C, Sack L. 2012. The determinants of leaf turgor loss point and prediction of drought tolerance of species and biomes: A global meta-analysis. Ecology Letters 15: 393–405.

Bauerle WL, Hinckley TM, Cermak J, Kucera J, Bible K. 1999. The canopy water relations of old-growth Douglas-fir trees. Trees - Structure and Function 13: 211–217.

Becker P, Meinzer FC, Wullschleger SD. 2000. Hydraulic limitation of tree height: A critique. Functional Ecology 14: 4–11.

Becker P, Tyree MT, Tsuda M. 1999. Hydraulic conductance of angiosperms versus conifers: similar transport sufficiency at the whole-plant level. Tree Physiology 19: 445–452.

Berry ZC, Smith WK. 2013. Ecophysiological importance of cloud immersion in a relic spruce-fir forest at elevational limits, southern Appalachian Mountains, USA. Oecologia 173: 637–648.

Bouche PS, Larter M, Domec J-C, Burlett R, Gasson P, Jansen S, Delzon S. 2014. A broad survey of hydraulic and mechanical safety in the xylem of conifers. Journal of Experimental Botany 65: 4419–4431.

Breshears DD, McDowell NG, Goddard KL, Dayem KE, Martens SN, Meyer CW, Brown KM. 2008. Foliar absorption of intercepted rainfall improves woody plant water status most during drought. Ecology 89: 41–47.

Brodribb TJ, Cochard H. 2009. Hydraulic failure defines the recovery and point of death in water-stressed conifers. Plant Physiology 149: 575–584.

Brodribb TJ, Feild TS, Jordan GJ. 2007. Leaf maximum photosynthetic rate and venation are linked by hydraulics. Plant Physiology 144: 1890–1898.

Brodribb TJ, Feild TS, Sack L. 2010. Viewing leaf structure and evolution from a hydraulic perspective. Functional Plant Biology 37: 488–498.

Brodribb TJ, Holbrook NM. 2005. Water stress deforms tracheids peripheral to the leaf vein of a tropical conifer. Plant Physiology 137: 1139–1146.

Brodribb TJ, Holbrook NM, Zwieniecki MA, Palma B. 2005. Leaf hydraulic capacity in ferns, conifers and angiosperms: impacts on photosynthetic maxima. New Phytologist, 165: 839–846.

Bucci SJ, Goldstein G, Meinzer FC, Scholz FG, Franco AC, Bustamante M. 2004. Functional convergence in hydraulic architecture and water relations of tropical savanna trees: from leaf to whole plant. Tree Physiology 24: 891–899.

Buckley TN. 2005. The control of stomata by water balance. New Phytologist 168: 275–292.

Burgess SSO, Dawson TE. 2004. The contribution of fog to the water relations of *Sequoia sempervirens* (D. Don): foliar uptake and prevention of dehydration. Plant, Cell and Environment 27: 1023–1034.

Burgess SSO, Pittermann J, Dawson TE. 2006. Hydraulic efficiency and safety of branch xylem increases with height in *Sequoia sempervirens* (D. Don) crowns. Plant, Cell &and Environment 29: 229–239.

Cavaleri MA, Oberbauer SF, Clark DB, Clark DA, Ryan G, Oberbauer F. 2010. Height is more in important than light determining in a forest leaf tropical morphology. Ecology 91: 1730–1739.

Cermak J, Kucera J, Bauerle WL, Phillips N, Hinckley TM. 2007. Tree water storage and its diurnal dynamics related to sap flow and changes in stem volume in old-growth Douglas-fir trees. Tree Physiology 27: 181–198.

Cheung YNS, Tyree MT, Dainty J. 1975. Water relations parameters on single leaves obtained in a pressure bomb and some ecological interpretations. Canadian Journal of Botany 53: 1342–1346.

Coble AP, Autio A, Cavaleri M a., Binkley D, Ryan MG. 2014. Converging patterns of vertical variability in leaf morphology and nitrogen across seven *Eucalyptus* plantations in Brazil and Hawaii, USA. Trees - Structure and Function 28: 1–15.

Cochard H, Froux F, Mayr S, Coutand C. 2004. Xylem wall collapse in water-stressed pine needles. Plant Physiology 134: 401–408.

Cowan IR. 1982. Regulation of water use in relation to carbon gain in higher plants. In: Lange OL, Nobel PS, Osmond CB, Ziegler H, Cowan IR eds. Physiological Plant Ecology II. Verlag Berlin・Heidelberg: Springer, 589–613.

Dawson TE. 1998. Fog in the California redwood forest: ecosystem inputs and use by plants. Oecologia 117: 476–485.

Demarty M, Morvan C, Thellier M. 1984. Calcium and the cell wall. Plant, Cell and Environment 7: 441–448.

Dokken KM, Davis LC, Marinkovic NS. 2005. Use of infrared microspectroscopy in plant growth and development. Applied Spectroscopy Reviews 40: 301–326.

Domec JC, Gartner BL. 2001. Cavitation and water storage capacity in bole xylem segments of mature and young Douglas-fir trees. Trees - Structure and Function 15: 204–214.

Du N, Fan J, Chen S. Liu Y. 2008. A hydraulic–photosynthetic model based on extended HLH and its application to coast redwood (*Sequoia sempervirens*). Journal of Theoretical Biology, 253, 393–400.

Dunand C, Tognolli M, Overney S, Tobel L Von, Meyer M De, Simon P, Penel C. 2002. Identification and characterisation of Ca^{2+}-pectate binding peroxidases in *Arabidopsis thaliana*. Journal of Plant Physiology 159: 1165–1171.

Dunham SM, Lachenbruch B, Ganio LM. 2007. Bayesian analysis of Douglas-fir hydraulic architecture at multiple scales. Trees- Structure and Function 21: 65–78.

Esau K. 1997. Anatomy of Seed Plants (2nd ed.). New York: John Wiley and Sons.

Evert RF. 2006. Esau's plant anatomy: meristems, cells, and tissues of the plant body: their structure, function, and development. John Wiley & Sons.

Franks PJ. 2006. Higher rates of leaf gas exchange are associated with higher leaf hydrodynamic pressure gradients. Plant, Cell and Environment 29: 584–592.

Godoy O, Gianoli E. 2013. Functional variation of leaf succulence in a cold rainforest epiphyte. Plant Ecology and Evolution 146: 167–172.

Gravel D, Canham CD, Beaudet M, Messier C. 2010. Shade tolerance, canopy gaps and mechanisms of coexistence of forest trees. Oikos 119: 475–484.

Hacke UG, Sperry JS. 2001. Functional and ecological xylem anatomy. Perspectives in Plant Ecology, Evolution and Systematics 4: 97–115.

Hacke UG. 2014. Irradiance-induced changes in hydraulic architecture. Botany 92: 437–442.

Heraud P, Caine S, Sanson G, Gleadow R, Wood BR, McNaughton D. 2007. Focal plane array infrared imaging: a new way to analyse leaf tissue. New Phytologist 173: 216–225.

Hinckley TM, Duhme F, Hinckley AR, Richter H. 1980. Water relations of drought hardy shrubs: osmotic potential and stomatal reactivity. Plant, Cell and Environment 3: 131–140.

Hiura T. 2001. Stochasticity of species assemblage of canopy trees and understory plants in a temperate secondary forest created by major disturbances. Ecological Research 16: 887–893.

Hu YS, Yao BJ. 1981. Transfusion tissue in gymnosperm leaves. Botanical Journal of the Linnean Society 83: 263–272.

Iogna P A, Bucci SJ, Scholz FG, Goldstein G. 2013. Homeostasis in leaf water potentials on leeward and windward sides of desert shrub crowns: Water loss control vs. high hydraulic efficiency. Oecologia 173: 675–687.

Ishii H. 2000. Canopy research using single-rope techniques in the temperate coniferous forests of the Pacific Northwest, USA. Japanese Journal of Ecology 50: 65-70.

Ishii H, Azuma W, Nabeshima E. 2013. The need for a canopy perspective to understand the importance of phenotypic plasticity for promoting species coexistence and light-use complementarity in forest ecosystems. Ecological Research 28: 191–198.

Ishii H, Hamada Y, Utsugi H. 2012. Variation in light-intercepting area and photosynthetic rate of sun and shade shoots of two *Picea* species in relation to the angle of incoming light. Tree Physiology 32: 1227–1236.

Ishii H, Jennings G, Sillett S, Koch G. 2008. Hydrostatic constraints on morphological exploitation of light in tall *Sequoia sempervirens* trees. Oecologia 156: 751–763.

Ishii H, Kitaoka S, Fujisaki T, Maruyama Y, Koike T. 2007. Plasticity of shoot and needle morphology and photosynthesis of two *Picea* species with different site preferences in northern Japan. Tree Physiology 27: 1595–1605.

Iwatsubo G. 1996. Forest Ecology (G Iwatsubo, Ed.). Buneido Co., Ltd.

Johnson DM, Meinzer FC, Woodruff DR, McCulloh KA. 2009. Leaf xylem embolism, detected acoustically and by cryo-SEM, corresponds to decreases in leaf hydraulic conductance in four evergreen species. Plant, Cell and Environment 32: 828–836.

Johnstone JA, Dawson TE. 2010. Climatic context and ecological implications of summer fog decline in the coast redwood region. Proceedings of the National Academy of Sciences of the United States of America 107: 4533–4538.

Koch GW, Sillett SC, Jennings GM, Davis SD. 2004. The limits to tree height. Nature 428: 851–854.

Koch GW, Sillett SC. 2009. A response to: limitations within “The limits to tree height”. American Journal of Botany 96: 545–547.

Kubiske ME, Abrams MD. 1991. Rehydration effects on pressure-volume relationships in four temperate woody species: variability with site, time of season and drought conditions. Oecologia 85: 537–542.

Lachenbruch B, McCulloh KA. 2014. Traits, properties, and performance: how woody plants combine hydraulic and mechanical functions in a cell, tissue, or whole plant. International Journal of Pharmaceutics: 747–764.

Laman TG. 1995. Safety Recommendations for Climbing Rain Forest Trees with “Single Rope Technique.” Biotropica 27: 406–409.

Larcher W. 2003. Physiological plant ecology: ecophysiology and stress physiology of functional groups. Berlin: Springer.

Larjavaara M. 2014. The world’s tallest trees grow in thermally similar climates. New Phytologist 202: 344–349.

Laur J, Hacke UG. 2013. Transpirational demand affects aquaporin expression in poplar roots. Journal of Experimental Botany 64: 2283–2293.

Laur J, Hacke UG. 2014. Exploring *Picea glauca* aquaporins in the context of needle water uptake and xylem refilling. New Phytologist 203: 388–400.

Liners F, Letesson JJ, Didembourg C, Van Cutsem P. 1989. Monoclonal antibodies against pectin: recognition of a conformation induced by calcium. Plant Physiology 91: 1419–1424.

Magnani F, Mencuccini M, Grace J. 2000. Age-related decline in stand productivity: The role of structural acclimation under hydraulic constraints. Plant, Cell and Environment 23: 251–263.

Marshall JD, Monserud RA. 2003. Foliage height influences specific leaf area of three conifer species. Canadian Journal of Forest Research 33: 164–170.

Martin TA, Hinckley TM, Meinzer FC, Sprugel DG. 1999. Boundary layer conductance, leaf temperature and transpiration of *Abies amabilis* branches. Tree Physiology 19: 435–443.

Martin CE, Willert DJ. 2000. Leaf epidermal hydathodes and the ecophysiological consequences of foliar water uptake in species of *Crassula* from the Namib Desert in southern Africa. Plant Biology 2: 229–242.

Martorell S, Diaz-Espejo A, Medrano H, Ball MC, Choat B. 2014. Rapid hydraulic recovery in *Eucalyptus pauciflora* after drought: linkages between stem hydraulics and leaf gas exchange. Plant, Cell and Environment 37: 617–626.

Martín-Gómez P, Barbeta a, Voltas J, Peñuelas J, Dennis K, Palacio S, Dawson TE, Ferrio JP. 2015. Isotope-ratio infrared spectroscopy: a reliable tool for the investigation of plant-water sources? New Phytologist 207: 914–917.

Maréchal Y. 2007. The hydrogen bond and the water molecule. Elsevier.

McCulloh K, Sperry JS, Lachenbruch B, Meinzer FC, Reich PB, Voelker S. 2010. Moving water well: Comparing hydraulic efficiency in twigs and trunks of coniferous, ring-porous, and diffuseporous saplings from temperate and tropical forests. New Phytologist 186: 439–450.

McDowell N, Barnard H, Bond BJ, Hinckley T, Hubbard RM, Ishii H, Kostner B, Magnani F, Marshall JD, Meinzer FC, Phillips N, Ryan MG, Whitehead D. 2002. The relationship between tree height and leaf area: sapwood area ratio. Oecologia 132: 12–20.

Meinzer F, McCulloh K, Lachenbruch B, Woodruff D, Johnson D. 2010. The blind men and the elephant: the impact of context and scale in evaluating conflicts between plant hydraulic safety and efficiency. Oecologia 164: 287–296.

Meinzer FC, Brooks JR, Domec J, Gartner BL, Warren JM, Woodruff DR, Bible K, Franco M, Sarg R. 2006. Dynamics of water transport and storage in conifers studied. Plant, Cell and Environment 29: 105–114.

Mencuccini M. 2003. The ecological significance of long-distance water transport: Short-term regulation, long-term acclimation and the hydraulic costs of stature across plant life forms. Plant, Cell and Environment 26: 163–182.

Mencuccini M, Martinez-Vilalta J, Vanderklein D, Hamid HA, Korakaki E, Lee S. Michiels B. 2005. Size-mediated ageing reduces vigour in trees. Ecology Letters 8: 1183–1190.

Midgley JJ. 2003. Is bigger better in plants? The hydraulic costs of increasing size in trees. Trends in Ecology and Evolution 18: 5–6.

Mullin LP, Sillett SC, Koch GW, Tu KP, Antoine ME. 2009. Physiological consequences of height-related morphological variation in *Sequoia sempervirens* foliage. Tree Physiology 29: 999–1010.

Nabeshima E, Hiura T. 2008. Size-dependency in hydraulic and photosynthetic properties of three *Acer* species having different maximum sizes. Ecological Research 23: 281–288.

Nakamoto K, Margoshes M, Rundle RE. 1955. Stretching frequencies as a function of distances in hydrogen bonds. Journal of the American Chemical Society 77: 6480–6486.

Negret BS, Perez F, Markesteijn L, Castillo MJ, Armesto JJ. 2013. Diverging drought-tolerance strategies explain tree species distribution along a fog-dependent moisture gradient in a temperate rain forest. Oecologia 173: 625–635.

Niinemets U, Kull O. 1995. Effects of light availability and tree size on the architecture of assimilative surface in the canopy of *Picea abies*: variation in needle morphology. Tree Physiology 15: 791–798.

Niinemets U. 2002. Stomatal conductance alone does not explain the decline in foliar photosynthetic rates with increasing tree age and size in *Picea abies* and *Pinus sylvestris*. Tree Physiology 22: 515–535.

Niinemets U. 2010. A review of light interception in plant stands from leaf to canopy in different plant functional types and in species with varying shade tolerance. Ecological Research 25: 693–714.

Oldham AR, Sillett SC, Tomescu AMF, Koch GW. 2010. The hydrostatic gradient, not light availability, drives height-related variation in *Sequoia sempervirens* (Cupressaceae) leaf anatomy. American Journal of Botany 97: 1087–1097.

Otoda T, Ishii H. 2009. Basal reiteration improves the hydraulic functional status of mature *Cinnamomum camphora* trees. Trees - Structure and Function 23: 317–323.

PRISM Climate Group Oregon State University. 2013. http://prism.oregonstate. edu.

Pallardy SG. 2007. Physiology of woody plants, 3rd edn. San Diego: Academic Press.

Parker WC, Colombo SJ. 1995. A critical re-examination of pressure-volume analysis of conifer shoots: comparison of three procedures for generating PV curves on shoots of *Pinus resinosa* Ait. seedlings. Journal of Experimental Botany 46: 1701–1709.

Peel MC, Finlayson BL, McMahon TA. 2007. Updated world map of the Köppen-Geiger climate classification. Hydrology and Earth System Sciences 11: 1633–1644.

Phillips N, Bond BJ, McDowell NG, Ryan MG, Schauer A. 2003. Leaf area compounds height-related hydraulic costs of water transport in Oregon White Oak trees. Functional Ecology 17: 832–840.

Phillips, Ryan MG, Bond BJ, McDowell NG, Hinckley TM, Cermak J. 2003. Reliance on stored water increases with tree size in three species in the Pacific Northwest. Tree Physiology 23: 237–245.

Prado K, Maurel C. 2013. Regulation of leaf hydraulics: from molecular to whole plant levels. Frontiers in Plant Science 4: 1–14.

Renninger HJ, Phillips N, Hodel DR. 2009. Comparative hydraulic and anatomic properties in palm trees (*Washingtonia robusta*) of varying heights: Implications for hydraulic limitation to increased height growth. Trees - Structure and Function 23: 911–921.

Ribeiro da Luz B. 2006. Attenuated total reflectance spectroscopy of plant leaves: A tool for ecological and botanical studies. New Phytologist 172: 305–318.

Richter H. 1978. A diagram for the description of water relations in plant cells and organs. Journal of Experimental Botany 29: 1197–1203.

Ritchie GA, Roden JR. 1985. Comparison between two methods of generating pressure-volume curves. Plant, Cell and Environment 8: 49–53.

Rodriguez P, Mellisho CD, Conejero W, Cruz ZN, Ortuno MF, Galindo A, Torrecillas A. 2012. Plant water relations of leaves of pomegranate trees under different irrigation conditions. Environmental and Experimental Botany 77: 19–24.

Ryan MG, Phillips N, Bond BJ. 2006. The hydraulic limitation hypothesis revisited. Plant, Cell and Environment 29: 367–381.

Ryan MG, Yoder BJ. 1997. Hydraulic limits to tree height and tree growth. Bioscience 47: 235–242.

Sack L, Cowan PD, Jaikumar N, Holbrook NM. 2003. The “hydrology” of leaves: co-ordination of structure and function in temperate woody species. Plant, Cell and Environment 26: 1343–1356.

Sack L, Holbrook NM. 2006. Leaf hydraulics. Annual Review of Plant Biology 57: 361–381.

Salleo S. 1983. Water relations parameters of two sicilian species of *Senecio* (groundsel) measured by the pressure bomb technique. New Phytologist 95: 179–188.

Scholz F, Phillips N, Bucci S, Meinzer F, Goldstein G. 2011. Hydraulic capacitance: biophysics and functional significance of internal water sources in relation to tree size. In: Meinzer FC, Lachenbruch B, Dawson TE, eds. Size- and Age-Related Changes in Tree Structure and Function. Springer, 341–361.

Schulte PJ, Hinckley TM. 1985. A comparison of pressure-volume curve data analysis techniques. Journal of Experimental Botany 36: 1590–1602.

Schulte PJ. 2012. Computational fluid dynamics models of conifer bordered pits show how pit structure affects flow. New Phytologist 193: 721–729.

Schulte PJ. 2012. Vertical and radial profiles in tracheid characteristics along the trunk of Douglas-fir trees with implications for water transport. Trees - Structure and Function 26: 421–433.

Sellin A, Kupper P. 2005. Effects of light availability versus hydraulic constraints on stomatal responses within a crown of silver birch. Oecologia 142: 388–397.

Sellin A, Kupper P. 2007. Temperature, light and leaf hydraulic conductance of little-leaf linden (*Tilia cordata*) in a mixed forest canopy. Tree Physiology 27: 679–88.

Sillett SC, Van Pelt R, Kramer RD, Carroll AL, Koch GW. 2015. Biomass and growth potential of *Eucalyptus regnans* up to 100m tall. Forest Ecology and Management 348: 78–91.

Simonin KA, Santiago LS, Dawson TE. 2009. Fog interception by *Sequoia sempervirens* (D. Don) crowns decouples physiology from soil water deficit. Plant, Cell and Environment 32: 882–892.

Sobrado MA. 2003. Hydraulic characteristics and leaf water use efficiency in trees from tropical montane habitats. Trees - Structure and Function 17: 400–406.

Sperry JS, Meinzer FC, McCulloh KA. 2008. Safety and efficiency conflicts in hydraulic architecture: scaling from tissues to trees. Plant, Cell and Environment 31: 632–645.

Stephenson NL, Das AJ, Condit R, Russo SE, Baker PJ, Beckman NG, Coomes DA, Lines ER, Morris WK, Ruger N, Alvarez E, Blundo C, Bunyavejchewin S, Chuyong G, Davies SJ, Duque A, Ewango CN, Flores O, Franklin JF, Grau HR, Hao Z, Harmon ME, Hubbell SP, Kenfack D, Lin Y, Makana JR, Malizia A, Malizia LR, Pabst RJ, Pongpattananurak N, Su SH, Sun IF, Tan S, Thomas D, van Mantgem PJ, Wang X, Wiser SK, Zavala MA. 2014. Rate of tree carbon accumulation increases continuously with tree size. Nature 507: 90–93.

Takeda H. 1931. A theory of “transfusion-tissue. Annals of Botany 27: 359–363.

Tsutsumi T. 1989. Forstry ecology (T Toshio, Ed.). Asakura Publishing Co., Ltd.

Tyree MT, Graham M, Cooper K, Bazos LJ. 1983. The hydraulic architecture of *Thuja occidentalis*. Canadian Journal of Botany 61: 2105–2111.

Tyree MT, Hammel HT. 1972. The measurement of the turgor pressure and the water relations of plants by the pressure-bomb technique. Journal of Experimental Botany 23: 267–282.

Tyree MT, Richter H. 1981. Alternative methods of analyzing water potential isotherms: some cautions and clarifications I. The impact of non-ideality and of some experimental errors. Journal of Experimental Botany 32: 643–653.

Tyree MT, Zimmermann MH. 2002. Xylem structure and the ascent of sap, 3rd edn. Springer-Verlag, Berlin.

Uemura A, Ishida A, Tobias D, Koike N, Matsumoto Y. 2004. Linkage between seasonal gas exchange and hydraulic acclimation in the top canopy leaves of *Fagus* trees in a mesic forest in Japan. Trees - Structure and Function 18: 452–459.

Valladares F, Niinemets U. 2007. The architecture of plant crowns: form design rules to light capture and performance. In: Pugnaire F, Valladares F. eds. Functional Plant Ecology. Taylor and Francis, New York. 101–149.

Watanabe S, Kojima K, Ide Y, Sasaki S. 2000. Effects of saline and osmotic stress on proline and sugar accumulation in *Populus euphratica* in vitro. Plant Cell, Tissue and Organ Culture 63: 199–206.

West GB, Brown JH, Enquist BJ. 1999. A general model for the structure, and algometry of plant vascular systems. Nature 400: 122–126.

Whitehead D, Jarvis PG, Waring RH. 1984. Stomatal conductance, transpiration, and resistance to water uptake in a *Pinus sylvestris* spacing experiment. Canadian Journal of Forest Research 14: 692–700.

Woodruff DR, Bond BJ, Meinzer FC. 2004. Does turgor limit growth in tall trees? Plant, Cell and Environment 27: 229–236.

Woodruff DR, Meinzer FC, Lachenbruch B. 2008. Height-related trends in leaf xylem anatomy and hydraulic characteristics in a tall conifer: safety versus efficiency in foliar water transport. New Phytologist 180: 90–99.

Xiloyannis C, Dichio B, Nuzzo V, Celano G. 1999. Defense strategies of olive against water stress. Acta Hort 474: 423–426.

Zaehle S. 2005. Effect of height on tree hydraulic conductance incompletely compensated by xylem tapering. Functional Ecology 19: 359–364.

Zhang Y-J, Rockwell FE, Wheeler JK, Holbrook NM. 2014. Reversible deformation of transfusion tracheids in *Taxus baccata* is associated with a reversible decrease in leaf hydraulic conductance. Plant Physiology 165: 1557–1565.

Zimmermann MH. 1983. Xylem Structure and the Ascent of Sap. Berlin: Springer.

Zimmermann MH, Milburn JA. 1982. Transport and storage of water. In: Lange OL, Nobel PS, Osmond CB, Ziegler H. eds. Physiological Plant Ecology II. Springer, Heidelburg. 135–151.

Zweifel R, Item H, Häsler R. 2000. Stem radius changes and their relation to stored water in stems of young Norway spruce trees. Trees - Structure and Function 15: 50–57.

要旨

“樹高の限界を決める要因は何か”という古くからの問いに対して、従来の定説では、樹冠上部が水不足に陥る水ストレスが主要因とされてきた（Hydraulic limitation hypothesis）。これは高木になるほど根から梢端部までの水輸送が物理的に困難となることに起因する。しかしその後の研究で、樹冠上部では葉が小型化して光合成が抑制されるため伸長が制限されることや、光合成に有利な枝先端部では通水性が高く水輸送が改善されることが報告され、水ストレスが直接的な樹高成長制限要因ではないことが示された。また、これらの報告では説明しきれていない、高所への水輸送の困難さを補償するメカニズムの存在が示唆されている。一方で、葉の小型化は樹高にともなう水ストレスの影響であるとも推測されてきた。しかし、樹高 50～100m にも達する高木の梢端にはアクセス困難であったため、葉が受けている水ストレスの実態は直接測定されず、理論的な推測に基づくものであった。本研究では、高木の梢端に Tree climbing の手法で登り、樹高成長を規定する生理学的要因について解明するため、葉の水分生理に関する様々な性質（水分特性）を直接的に測定し、高木の葉がうける水ストレスの実態と適応戦略について明らかにした。

第 1 章では、（１）樹高成長研究の生態学、林業的意義、（２）高木の樹高成長についての既往研究、（３）水分生理特性と形態解剖学的特性の関係について説明し、本研究の構成を概説した。

第 2 章では、現存する世界一高い種であるセコイアメスギ（*Sequoia sempervirens*）において、高所への水輸送の物理的制限が、葉内における貯水によって部分的に補償されることを明らかにした。北米カルフォルニア州の湿潤な北部地域（最大樹高約 100m）と乾燥した南部地域（最大樹高約 80m）において、セコイアメスギの梢端から最下枝まで樹冠内の様々な高さの葉の水分生理特性を測定した結果、葉が受ける水ストレスの指標（萎れ時の葉の水ポ

テンシャル）は樹冠内の高さや光環境によらず一定であった。一方、葉の貯水性が高さにともない増加した。また、高さにともなう葉の小型化によって、受光面積が小さくなり、光合成においては不利になる一方、葉の蒸散面積に対する貯水量が増加し、水分保持においては有利な形態である事が示された。その結果、樹冠上部で物理的に生じる水不足の影響は、葉の高い貯水性によって補償されることが示唆された。セコイアメスギにおいては、気象条件の異なる地域間で同様の結果が得られ、日中の蒸散量の 5 倍に相当する貯留水を葉が有することが示された。また、葉横断面の解剖特性を解析した結果、裸子植物に特有の Transfusion 組織の断面積が高さにともない増加していたことから、同組織の貯水への貢献が示唆された。一方で、木部組織の横断面積は減少していたことから、セコイアメスギの高所の葉は根からの水分供給よりも霧や朝露の貯留水に依存するところが大きいことが示唆された。

第 3 章では、日本最大級の樹高約 50m の秋田スギ（*Cryptomeria japonica*）において、Transfusion 組織が、葉での水需要の日変化に応じて、細胞の形状が変化するとともに水の貯留場および供給源として機能することを明らかにした。梢端から最下枝まで樹冠内の様々な高さの葉の水分生理特性および形態解剖学的特性を測定した結果、セコイアメスギと同様の傾向が得られた。さらに、スギの樹上で葉を液体窒素により低温凍結し、低温走査顕微鏡（cryo-SEM）により内部の組織と水を同時に観察すると、Transfusion 組織は日中に水分を含んだまま細胞の形状が収縮して扁平に変形し、夜明け前には再水和して元の形状を示した。つまり、Transfusion 組織ではスポンジのように細胞の可逆的な形状変化とともに水の出入りが生じ、水分貯留および日中の給水源を担うことが示唆された。樹冠内の水分恒常性には、このような葉の組織構造の変化が寄与すると考えられる。

第 4 章では、高木の葉の水分保持メカニズムに迫るために、第 3 章と同様の調査木において、岩石や木材など無機物を対象に利用されている赤外分光法と顕微鏡をかけあわせた顕微赤外分光法を、葉横断面に適用する実験系を確立した。葉横断面のスペクトルから得られた水分量は、生理学的測定と同様、高さにともない増加していた。また、葉横断面のスペ

クトルから得られた糖類全般の量は高さにともない増加する一方で、生理学的測定において葉の浸透調節能力は高さによらず一定であったことから、高さにともない増加するのは親水性の多糖類、たとえば水和するとゲル状になるペクチンなどであることが示唆された。そして、スペクトルマッピングによって、水・糖類等の葉横断面における面的定量が可視化できた。高所の葉は水・多糖類の分布が Transfusion 組織以外に葉肉組織中にも拡大していることが明らかとなり、葉における水の保持メカニズムに多糖類が寄与することが想定された。

第 5 章では、以上の結果をまとめ、水輸送の物理的制限に基づく既往の樹高成長制限仮説にはなかった、高木における水ストレスへの適応という新しい観点から、水分恒常性仮説（Hydraulic homeostasis hypothesis）を示した。高さにともなう葉の貯水能力の増加によって樹冠内の水分恒常性が実現され、梢端の生理機能は維持される一方、そのような高い貯水能力を実現する組織構造の変化は光合成能力に寄与する組織構造と資源配分の観点からトレードオフの関係にあるため、樹高成長は葉における両機能のバランスによって規定されると考えられる。今後の樹高成長の規定要因の解明では、環境などの物理的制限要因の影響のみならず、樹木による適応的な補償メカニズムの存在にも同時に注目するべきである。

Acknowledgments

I was able to complete my doctoral dissertation with supports by many people. I am grateful to all of them.

I thank my supervisor, Associate Prof. Hiroaki Ishii in the Laboratory of Forest Resources, Kobe University. He always supported and advised me all investigates in fields and the writing for journals. He is a great mentor and master of tree-climbing for me. I am also grateful to his family, Keiko, Hikaru and Konomi, for their kindness during the expedition.

I would like to appreciate Prof. Keiko Kuroda in the Laboratory of Forest Resources, Kobe University. She had always been actively interested in my work and provided valuable advises. I was taught various anatomical techniques by her.

Prof. Stephen C. Sillett in Humboldt State University, USA, who is a great pioneer for research in tall *S. sempervirens* with rope techniques supported me the investigate in tall *S. sempervirens*. He also co-analyzed and co-wrote for journals about the study of *S. sempervirens*. He and his wife Ms. Marie Antoine let me do a homestay, supported my local life, and encouraged me. I would like to appreciate all of their kindness, supports and advices. I also thank Mrs. Robert Van Pelt, Jim Campbell-Spickler, Giacmo Renzro, Russell D. Kramer, Anthony Ambrose, Cameron Williams, and Ms. Allyson L. Carroll for supporting and advising me to my study in *Sequoia sempervirens*.

I thank Drs. A. Makita, K. Takata, K. Hoshizaki, and M. Matsushita of Akita Pref. University for facilitating the study and Mss. Kana Hotta, Misako Nakatani, Ayumi Shiraki and Mr. Takuya Minamino of the Laboratory of Forest Resources, Kobe

University for field assistance. On the coattails of them, I was able to investigate it in Akita. Special thanks to Mrs. Sakagami and Yusaku Sasabe who is a tree doctor and arborist for field assistance.

Prof. Satoru Nakashima in Osaka university all supported the study by using infrared micro-spectroscopic. I really thank for his kind and careful instruction though I am the student of other university. I also thank Ms. Hiromi Ogawa and Ms. Eri Yamakita also for supporting the experiment. Special thanks to Ms. Rika Harui of Thermo Fisher Scientific for her supports on the IR mapping measurements.

The study in chapter 2 was supported by the Save-the-Redwoods League, the Kenneth L. Fisher Chair in Redwood Forest Ecology at Humboldt State University, JSPS (KAKENHI #23380085 and #20780118), HUMAP and Hyogo STA. I thank the California Department of Parks and Recreation and Landels-Hill Big Creek Reserve for permission to conduct the research. The study in chapter 3 and chapter 4 was supported by JSPS Research Fellow (#02502390) and JSPS Kakenhi (#23380085). I thank the Noshiro Education Board and Tohoku Forest Management Office, Ministry of Agriculture, Forestry and Fisheries for permission to conduct the research. I am grateful to them for financial supports.

Finally, I am extremely grateful to great members of the Laboratory of Forest Resources, Kobe University who discussed about my research and spent precious times together. I am also thanks to my friend who encouraged me. My parents and sister always supported and encouraged me over the years. Their kind support provided me with driving force of my research and wide experience of my daily life.